IDO—22058

PROBABLE HYDROLOGIC EFFECTS OF A HYPOTHETICAL FAILURE OF MACKAY DAM ON THE BIG LOST RIVER VALLEY FROM MACKAY, IDAHO, TO THE IDAHO NATIONAL ENGINEERING LABORATORY

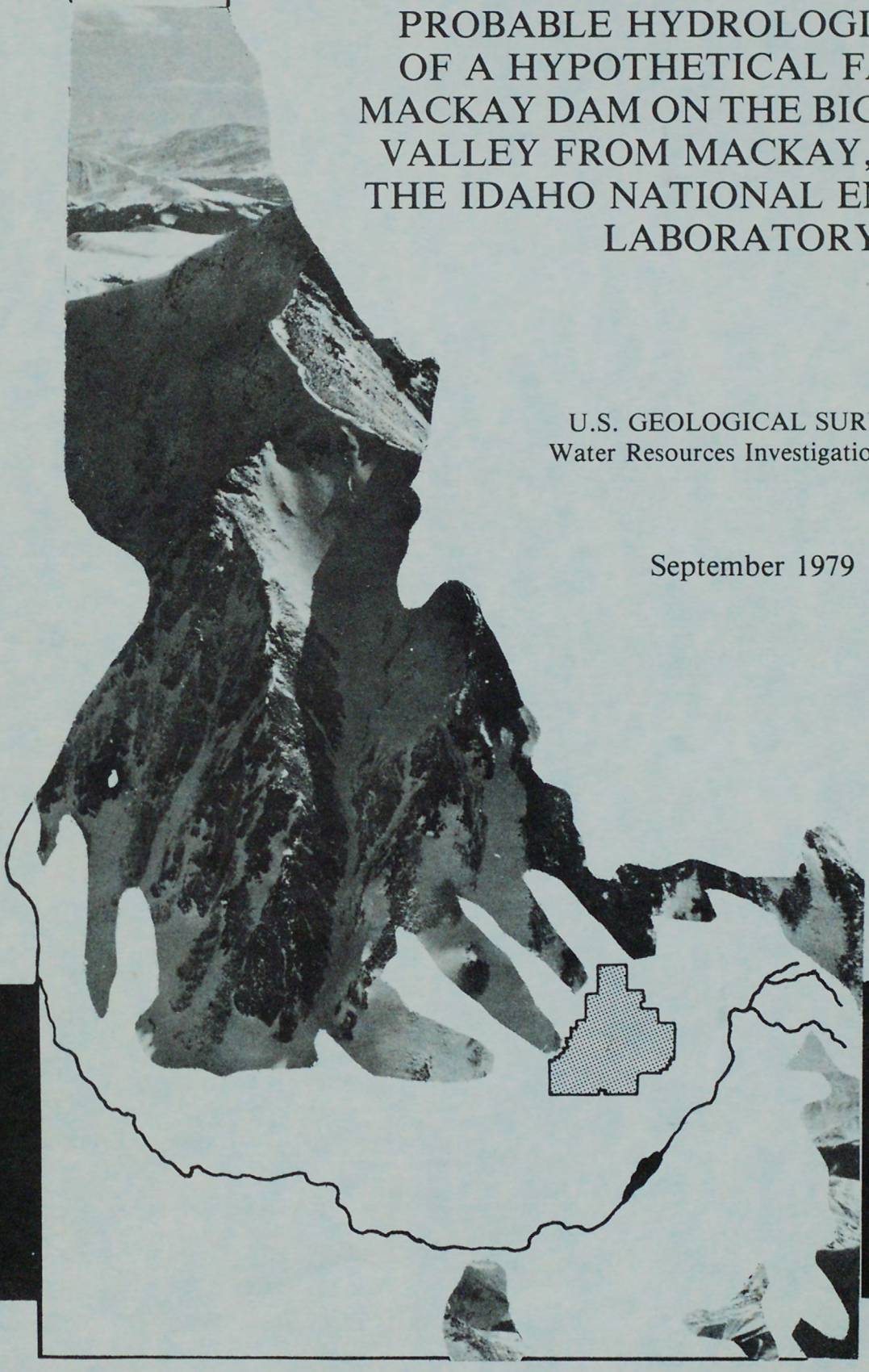

U.S. GEOLOGICAL SURVEY
Water Resources Investigation 79-99

September 1979

PREPARED FOR THE U.S.
DEPARTMENT
OF ENERGY

50272-101

REPORT DOCUMENTATION PAGE	1. REPORT NO.	2.	3. Recipient's Accession No.

4. Title and Subtitle

PROBABLE HYDROLOGIC EFFECTS OF A HYPOTHETICAL FAILURE OF MACKAY DAM ON THE BIG LOST RIVER VALLEY FROM MACKAY, IDAHO, TO THE IDAHO NATIONAL ENGINEERING LABORATORY

5. Report Date: September 1979

6.

7. Author(s)

Leroy Druffel, Gloria J. Stiltner, and Thomas N. Keefer

8. Performing Organization Rept. No. USGS/WRI-79-99

9. Performing Organization Name and Address

U.S. Geological Survey, Water Resources Division
Gulf Coast Hydroscience Center
National Space Technology Laboratories
NSTL Station, Mississippi 39529

10. Project/Task/Work Unit No.

11. Contract(C) or Grant(G) No.
(C)
(G)

12. Sponsoring Organization Name and Address

U.S. Geological Survey, Water Resources Division
P. O. Box 2230
INEL, CF 690, Room 164
Idaho Falls, Idaho 83401

13. Type of Report & Period Covered: Final

14.

15. Supplementary Notes

These studies have been sponsored and funded by the U.S. Department of Energy.

16. Abstract (Limit: 200 words)

Mackay Dam is an irrigation reservoir on the Big Lost River, Idaho, approximately 7.2 kilometers northwest of Mackay, Idaho. Consequences of possible rupture of the dam have long concerned the residents of the river valley. The presence of reactors and management complex for nuclear wastes on the reservation of the Idaho National Engineering Laboratory (INEL), near the river, gives additional cause for concern over the consequences of a rupture of Mackay Dam.

The objective of this report is to calculate and route the flood wave resulting from the hypothetical failure of Mackay Dam downstream to INEL. Both a full and a 50 percent partial breach of this dam are investigated. Two techniques are used to develop the dam-break model. The method of characteristics is used to propagate the shock wave after the dam fails. The linear implicit finite-difference solution is used to route the flood wave after the shock wave has dissipated.

The time of travel of the flood wave, duration of flooding, and magnitude of the flood are determined for eight selected sites from Mackay, Idaho, through the INEL diversion. At 4.2 kilometers above the INEL diversion, a maximum discharge of 1,503 and 1,275 cubic meters per second were calculated for the full and partial breach, respectively.

17. Document Analysis a. Descriptors

*Dam failure, *Flood routing, *Unsteady flow, *Mathematical models, Depth, Discharge, Computer models, Gradually varied flow, Open-channel flow, Hydrographs

b. Identifiers/Open-Ended Terms

*Dam break, *Mackay Dam, Shock waves, Method of characteristics, Linearized implicit finite-difference scheme, Nonprismatic channels

c. COSATI Field/Group

18. Availability Statement	19. Security Class (This Report)	21. No. of Pages
No restriction on distribution.	UNCLASSIFIED	53
	20. Security Class (This Page) UNCLASSIFIED	22. Price

PROBABLE HYDROLOGIC EFFECTS OF A HYPOTHETICAL FAILURE OF MACKAY DAM ON THE BIG LOST RIVER VALLEY FROM MACKAY, IDAHO, TO THE IDAHO NATIONAL ENGINEERING LABORATORY

By Leroy Druffel, Gloria J. Stiltner, and Thomas N. Keefer

U.S. GEOLOGICAL SURVEY

Water-Resources Investigations 79-99

Prepared for the U.S. Department of Energy

September 1979

UNITED STATES DEPARTMENT OF THE INTERIOR

CECIL D. ANDRUS, Secretary

GEOLOGICAL SURVEY

H. William Menard, Director

For additional information write to:

U.S. Geological Survey, WRD
Gulf Coast Hydroscience Center
National Space Technology Laboratories
NSTL Station, Mississippi 39529

CONTENTS

ILLUSTRATIONS

TABLES

CONVERSION FACTORS

For use of those readers who may prefer to use inch-pound units rather than metric units, the conversion factors for the terms used in this report are listed below:

Multiply metric unit	By	To obtain inch-pound unit
cubic hectometer (hm^3)	811.03	acre-foot (acre-ft)
cubic meter (m^3)	0.000811	acre-foot (acre-ft)
cubic meter per second (m^3/s)	35.314	cubic foot per second (ft^3/s)
hectare (ha)	2.471	acre
kilometer (km)	0.6214	mile (mi)
meter (m)	3.2808	foot (ft)
square kilometer (km^2)	0.3861	square mile (mi^2)

PROBABLE HYDROLOGIC EFFECTS OF A HYPOTHETICAL FAILURE OF MACKAY DAM ON THE BIG LOST RIVER VALLEY FROM MACKAY, IDAHO, TO THE IDAHO NATIONAL ENGINEERING LABORATORY

By Leroy Druffel, Gloria J. Stiltner, and Thomas N. Keefer

ABSTRACT

Mackay Dam is an irrigation reservoir on the Big Lost River, Idaho, approximately 7.2 kilometers northwest of Mackay, Idaho. Consequences of possible rupture of the dam have long concerned the residents of the river valley. The presence of reactors and of a management complex for nuclear wastes on the reservation of the Idaho National Engineering Laboratory (INEL), near the river, give additional cause for concern over the consequences of a rupture of Mackay Dam.

The objective of this report is to calculate and route the flood wave resulting from the hypothetical failure of Mackay Dam downstream to the INEL. Both a full and a 50 percent partial breach of this dam are investigated. Two techniques are used to develop the dam-break model. The method of characteristics is used to propagate the shock wave after the dam fails. The linear implicit finite-difference solution is used to route the flood wave after the shock wave has dissipated.

The time of travel of the flood wave, duration of flooding, and magnitude of the flood are determined for eight selected sites from Mackay Dam, Idaho, through the INEL diversion. At 4.2 kilometers above the INEL diversion, peak discharges of 1,502 and 1,275 cubic meters per second and peak flood elevations of 1,550.3 and 1,550.2 meters were calculated for the full and partial breach, respectively. Flood discharges and flood peaks were not compared for the area downstream of the diversion because of the lack of detailed flood plain geometry.

INTRODUCTION

Mackay Dam is an earthfill dam, 24.38 m high and approximately 600 m long at dam crest on the Big Lost River 7.2 km northwest of Mackay, Idaho. The reservoir behind Mackay Dam contains 54.7 hm^3 of water at spillway crest. Consequences of possible rupture of the dam have concerned the residents of the river valley ever since construction began in 1905. Fear of rupture was heightened by a high leakage rate beneath the dam. This leakage varied from 1.4 m^3/s at minimum storage to as much as 4.8 m^3/s at maximum storage. The leakage has slowly

decreased since construction was completed in 1918. Consequences of possible failure due to seismic activity are another concern. The dam rests on a fault which bounds the central mass of the White Knob Mountains. The presence of a limestone mass forming the right abutment of the dam is related to this fault (Crosthwaite and others, 1970). These facts influenced the decision to limit the height of the dam to 22.88 m rather than the original 36 m design value. However, because of increased demand for water, crest of the spillway and the dam were raised 1.5 m in 1956, bringing it to the 24.38 m height. This renewed concern about failure.

The Idaho National Engineering Laboratory (INEL) is located in a 2,315 km^2 area which includes the downstream end of the Big Lost River. It is approximately 72 km from Mackay Dam to the western boundary of the laboratory site. The river valley and INEL area are shown in figure 1. In addition to various test areas for nuclear reactors, the INEL site contains a Radioactive Waste Management Complex (RWMC) for the nuclear wastes. The RWMC is located approximately 3 km south of the river by the INEL diversion. The presence of the RWMC and the reactor facilities in close proximity to the river gives additional concerns for the consequences of possible rupture of Mackay Dam.

The objective of this report is to route the flood wave resulting from the hypothetical failure of Mackay Dam. Specifically, the time of travel of the flood wave, duration of flooding, and magnitude of flood flow for selected sites on the river are determined. The steady discharge in the Big Lost River the instant before failure is assumed to be the largest flood of record, 85 m^3/s. Both a complete and a 50 percent partial failure of the dam are investigated.

LITERATURE REVIEW

Dam-break models have been developed based on the gradually varied unsteady flow equations or the shock wave equations.

Price and others (1974) compared the dam-break equations developed by Saint Venant to the results from an explicit finite-difference solution to the gradually varied unsteady flow equations. Saint Venant's equations compute the discharge and the depth at which the discharge will occur. The equations are

$$Q = \frac{8}{27} B \sqrt{g} h^{3/2} \text{ and } y = 4/9 h \quad (1)$$

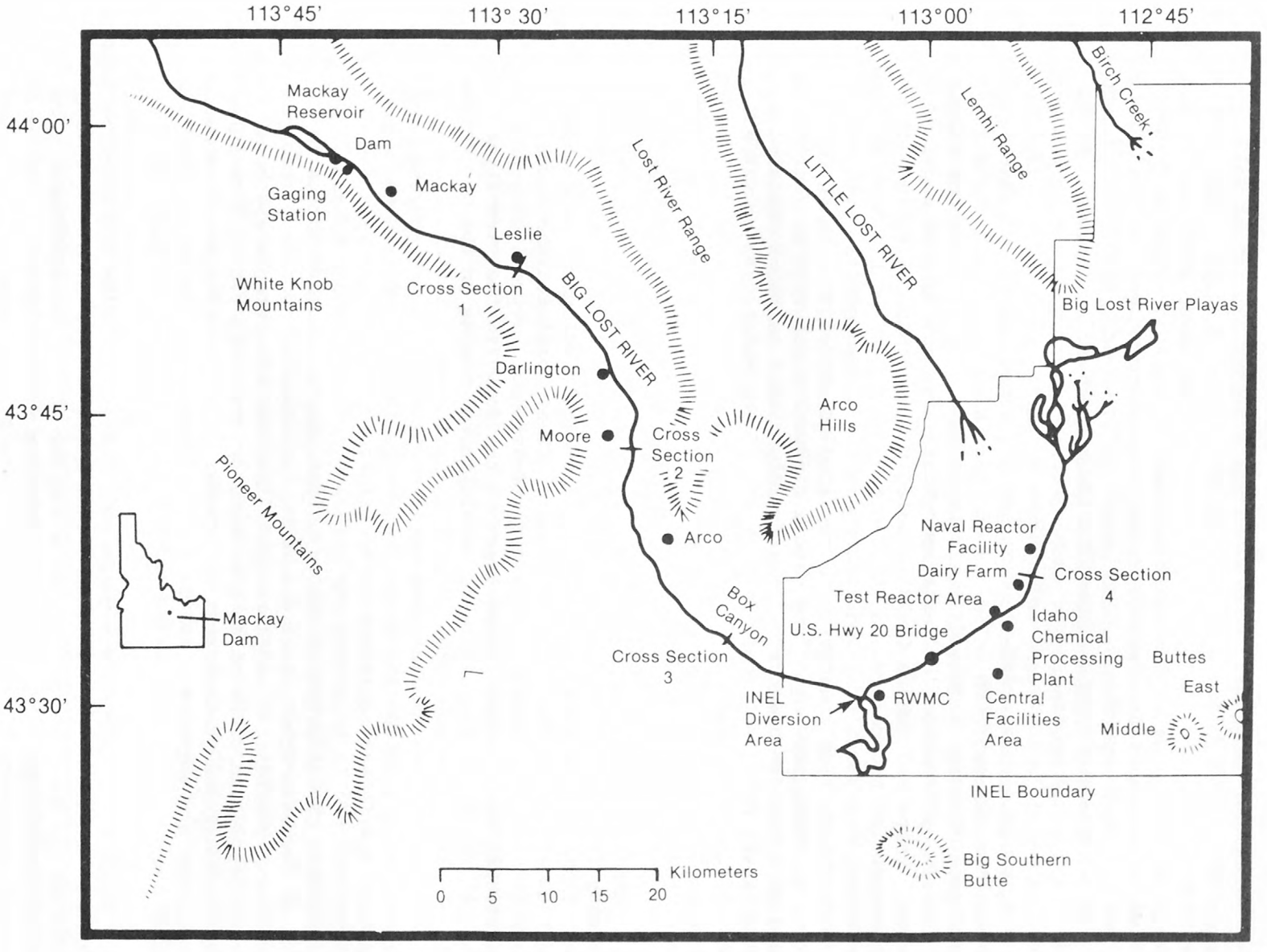

Figure 1.--Location of sites in the Big Lost River basin downstream from Mackay Reservoir.

where,

Q = discharge at dam cross section,
B = width of dam cross section,
h = depth upstream of dam, and
y = depth corresponding to the peak discharge at the dam cross section.

This equation was developed assuming a frictionless, prismatic, rectangular channel with unlimited storage in the reservoir and a dry downstream channel. Although it is impossible to find these conditions in a field application, the equation should give an order of magnitude answer. Price and others (1974) studied the hypothetical failure of a dam connecting two reservoirs and concluded that the peak discharge from the unsteady gradually varied flow equations agreed closely with the peak discharge from equation 1. They also concluded that the gradually varied unsteady flow equations gave a reasonable solution to routing the flood from the dam break after the rapidly varied parts of the flow (shock wave) had dissipated. A weakness of the model used by Price is that it cannot compute supercritical flow, and, if a partial failure or contracted full failure was simulated, the model used a critical depth rating curve at the dam as a boundary condition.

Gundlack and Thomas (1977) applied a similar gradually varied unsteady flow model to the Teton Dam break. They investigated the sensitivity of the breach size, rate of breach development, and channel roughness value to the computed results. They concluded that none of the parameters investigated were very significant in predicting peak elevations, 8 km or more, downstream of the dam. In the vicinity of the dam, the depth and velocity were sensitive to changes in the parameters. This model has the same problem with computing supercritical flow as Price's model. Because accurate water-surface elevations and discharges were not available for the Teton Dam break, the modeled results of Gundlack and Thomas could not be verified.

Sakkas (1974) presents dimensionless graphs to solve for arrival time of the wave front, peak elevation, and time of occurrence of peak elevation at arbitrary sections below the dam. The graphs are based on a characteristics solution to the unsteady gradually varied flow equations. The reservoir and channel must be prismatic, of constant roughness and slope, and dry downstream of the dam. Because of these restrictions, the answers must be considered approximate for any field application.

Levin (1952) presents a graphical method of solving for water-surface profiles upstream and downstream of the breached dam. The method is based on the Saint Venant equations and the shock wave equations. The method worked well when compared to results from a physical model. However, the method would be tedious to apply to a large reservoir and river system.

Flow conditions during a dam break under the usual assumption of instantaneous dam failure include a shock wave and supercritical and subcritical flow downstream of the dam. Dam-break models currently used by the U.S. Army Corps of Engineers and Tennessee Valley Authority are identical, at least conceptually, to the gradually varied flow models used by Price and others (1974) and Gundlack and Thomas (1977). The models cannot correctly handle these flow phenomena. However, after the shock wave has dissipated, although some regions of rapidly varied flow will still exist, the gradually varied flow equations will probably give reasonable dam-break flood routing results. This conclusion is supported by Martin and DeFazio (1969) and Cunge (1975), who have observed that the numerical solution to the gradually varied flow equations can pass through regions of rapidly varied flow and give a reasonable overall solution.

A general dam-break model should simulate the shock wave, account for the possibility of subcritical or supercritical flow, and be applicable to natural, nonprismatic channels. This could be accomplished by a combination of models: one model that would properly describe the translation and dissipation of the shock wave, and a gradually varied flow model to continue routing the dam-break flood wave after the shock has dissipated. This was the approach taken in this paper.

THE DAM-BREAK MODEL

The Equations

The processes involved in failure of a dam include the failure of the structure, acceleration of the water in the reservoir, formation of the shock wave, and after the shock wave has dissipated, propagation of the flood wave.

How the dam structurally fails determines the size, shape, and development rate of the break. These factors determine the peak outflow rate and thus the maximum elevation and discharges that will be obtained downstream of the dam. Unfortunately, the mechanics of the development of the dam breach are not available. However, for planning purposes, the worst possible failure is assumed. An instantaneous breach of the entire dam will give the maximum flood at INEL. Instantaneous partial failures of arbitrary shape can also be used to show the sensitivity of the downstream elevations and velocities to the breach size and shape. In this report a complete breach and a partial, trapezoidal breach were used.

At the moment of failure, a discontinuity exists in the water surface at the dam. An instant later, a shock wave develops and progresses downstream (Stoker, 1957). Using the laws of conservation of mass and momentum, the Rankine-Hugoniot shock wave equations can be developed.

The equations are:

$$\dot{\xi} = \frac{A_L V_L - A_R V_R}{A_L - A_R} \tag{2}$$

where,

$\dot{\xi}$ = velocity of the shock wave,
A_L = cross-sectional area to the left of the shock wave,
V_L = mean stream velocity to the left of the shock wave,
A_R = cross-sectional area to the right of the shock wave, and
V_R = mean stream velocity to the right of the shock wave.

$$V_L = V_R - (A_L - A_R)\left[\left(\frac{g}{A_L A_R}\,\frac{A_L \bar{h}_L - A_R \bar{h}_R}{A_L - A_R}\right)\right]^{1/2} \tag{3}$$

where,

g = acceleration due to gravity,
$\bar{h}_L$ = depth of cross-sectional area of flow centroid to left of shock wave, and
$\bar{h}_R$ = depth of cross-sectional area of flow centroid to right of shock wave.

If three of the five unknowns in equations 2 and 3 are known, then the remaining two can be determined by solution of equations 2 and 3. The use of the shock equations in the unsteady flow model will be discussed later.

As the shock wave progresses downstream, energy losses will cause the discontinuity to dissipate and the flow in the entire system can be described by the gradually varied, unsteady flow equations. The equations are:

$$\frac{\partial A}{\partial t} + \frac{\partial Q}{\partial x} = q \tag{4}$$

where,

A = cross-sectional area of flow normal to the flow direction, x,
Q = discharge passing through the cross-sectional area of flow, and
q = lateral inflow per unit length of channel.

$$\frac{\partial u}{\partial t} + u\frac{\partial u}{\partial x} + g\left(\frac{\partial y}{\partial x} + \frac{\partial z}{\partial x} + S_F\right) = D_L \qquad (5)$$

where,

u = mean flow velocity in x direction,
y = flow depth,
z = bed elevation,
S_F = resistance slope, and
D_L = factor to account for flow changes due to lateral inflow or outflow.

Equations 4 and 5 are applicable to unsteady, spacially varied flow in a rigid channel of arbitrary shape. Strelkoff (1969) gives an excellent presentation of these equations.

With equations 2 through 5, a one-dimensional solution to the dam-break problem can be developed. The validity of the equations has been proven and can be accepted as adequate for this modeling effort.

The Solution

Assuming the equations to be solved are adequate, the method of solution must be selected. Two methods were used in this study, each having advantages for particular situations.

The first technique is an explicit MOC (method of characteristics) solution with specified time intervals. The MOC solution has traits which make it possible to link the shock wave equations with the gradually varied flow equations. Chen (1975) couples these equations. The flow is divided into the rapidly varied region at the shock wave, and two gradually varied regions on either side of the shock wave. The model advances the shock wave from its previous position using the following equation:

$$X' = X + \dot{\xi}\,\Delta t \qquad (6)$$

where,

$\dot{\xi}$ = velocity of the shock wave,
X' = new location of the shock wave at time, $t + \Delta t$,
X = location of the shock at time, t, and
Δt = time step.

When the position of the shock is known, equations 2 and 3 along with three characteristic equations from the adjacent gradually varied flow region are used to compute the new values of $\dot{\xi}$, V_L, V_R, A_L, and A_R. The velocities and depths in the gradually varied flow regions on

either side of the shock wave are then computed using the MOC solution to equations 4 and 5. MOC solution converts equations 4 and 5 into two characteristics equations which apply along the characteristic curves. The characteristic equations can be solved at the intersection of the characteristic curves for the flow depth and velocity. Chen (1975) presents the characteristic curves, characteristic equations, and the explicit, specified interval solution algorithm used to solve them. The computer model presented by Chen (1975) was modified by Chen (oral commun., 1977) to allow for generating initial conditions for the reservoir and stream and nonprismatic cross sections.

The second technique used in this report is an IFD (linear implicit, finite-difference) solution to equations 4 and 5. Finite-difference approximations based on a four-point grid in the time and space plane replaces the partial derivatives in equations 4 and 5. The spacial derivatives are fully forward in time and centered in space while the time derivatives are centered in both time and space. The equation is linearized by expressing the nonlinear multipliers of the space derivatives on the known time level. Algebraic manipulation of the finite-difference equations result in two linear equations, each with four unknowns.

With known upstream and downstream boundary conditions, a matrix of linear equations can be formed and solved implicitly for the depths and velocities at specified cross sections.

Strelkoff (1970) and Bennett (1975) presented the development of the IFD method and the advantages of its use for solving equations 4 and 5. With some modification, the solution they presented is used in the computer model used in this project. The most important modification was an alternate method of writing the finite-difference form of the time derivatives for equations 4 and 5 suggested by Chen (oral commun., 1977). Strelkoff (1970) and Bennett (1975) centered the time derivative in space and time as indicated in figure 2. In order to make the method more stable in rapidly varied flow, the time derivative was rewritten in a diffusive form. Using figure 2 as a guide, the difference equation would normally use f_i^j and f_{i+1}^j on the known time line and f_i^{j+1} and f_{i+1}^{j+1} on the unknown time line to compute the space and time centered time derivative, that is,

$$\left.\frac{\partial F}{\partial t}\right|_{i+1}^{j+1} = \frac{1}{2\Delta t}\left\{f_i^{j+1} - f_i^j + f_{i+1}^{j+1} - f_{i+1}^j\right\} \qquad (7)$$

However, the time derivative was rewritten so a weighted average of f_{i-1}^j, f_i^j, and f_{i+1}^j was used to compute f_i^j; and f_i^j, f_{i+1}^j, and

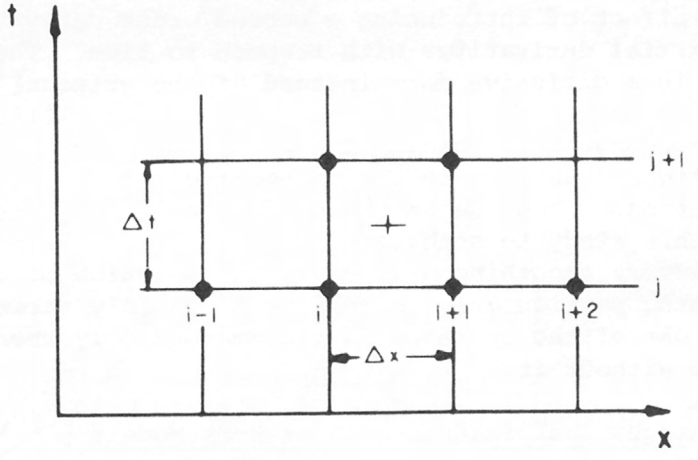

Figure 2.--Grid to form difference equation for time derivative.

f^j_{i+2} were used to compute f^j_{i+1}. The difference form of the derivative was then:

$$\left.\frac{\partial F}{\partial t}\right|^{j+1/2}_{i+1/2} = \frac{1}{2\Delta t}\left\{f^{j+1}_i - \left[(1-\alpha)\, f^j_i + \frac{\alpha}{2}\left(f^j_{i+1} + f^j_{i-1}\right)\right]\right.$$

$$\left. + f^{j+1}_{i+1} - \left[(1-\alpha)\, f^j_{i+1} + \frac{\alpha}{2}\left(f^j_{i+2} + f^j_i\right)\right]\right\} \qquad (8)$$

in which α is the diffusive weighting factor. If α is equal to zero, the scheme is identical to Strelkoff (1970) and Bennett (1975). If α is equal to one, the scheme is said to be fully diffusive. A weighting factor of 0.5 was used in this study. The scheme is similar to an explicit diffusive scheme mentioned by Liggett and Cunge (1975). Both schemes have the effect of introducing a second order derivative in the equations with partial derivatives with respect to time. The resulting equation is then in a diffusive form instead of the original convective form. The diffusive form of the equation smooths instabilities that would occur in the convective form. Figure 3 is an example of the IFD solution of equations 4 and 5 with the convective and the diffusive forms of the equations. The use of the diffusive form of the equation was valuable in this study to stabilize the IFD scheme for use in rapidly varied flow. However, smoothing will cause the solution of the equations to be less accurate, particularly in regions of rapidly varied flow. For this reason, use of the operator is recommended only when the solution would be unstable without it.

Advantages and Disadvantages of Both Models

The MOC and IFD models each have advantages for certain applications. The MOC model's primary advantage is the ability to link the gradually varied flow equations to the shock wave equations and thus be able to propagate the shock wave after the dam fails. The IFD model cannot handle this discontinuity through the dam. The MOC model was used from the instant of failure until the shock wave front dissipated all the shock energy. Although the MOC solution is accepted as the most accurate for the gradually varied, unsteady flow equations, the MOC has some disadvantages as programed in the current model used in this report. The most significant disadvantage is the limitation of the time step increment by the Courant conditions for stability (Courant and others, 1928). This requires small time increment, and consequently, a large number of time steps to complete a given simulation period. Another slight disadvantage is the complexity of the computer program required to solve the MOC equations. The characteristic lines do not intersect the time and space grid at specified points unless provisions are made

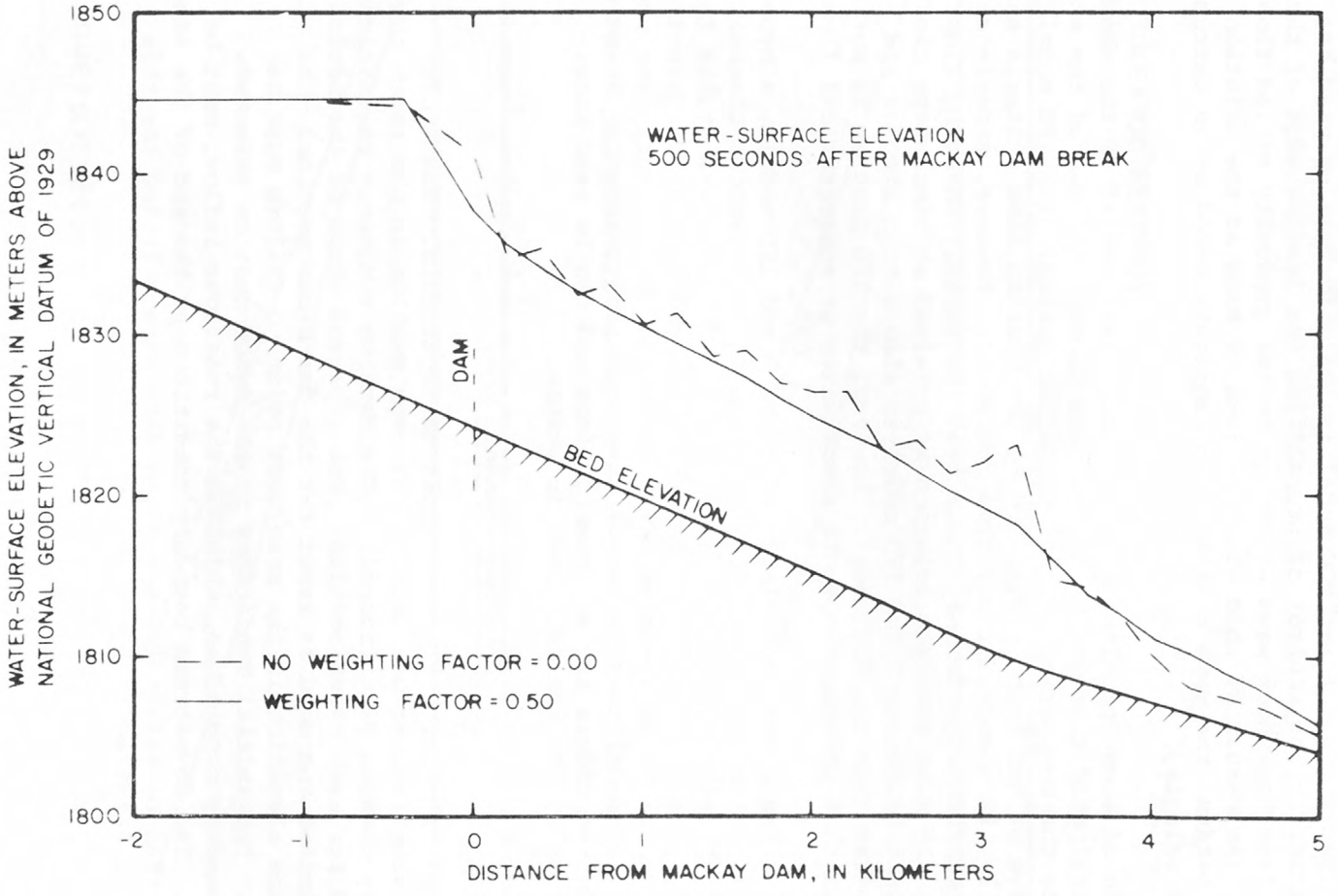

Figure 3.--Implicit finite-difference solution with and without diffusive weighting factor.

in the formulation and programing of the model. For these reasons, it would be cost prohibitive to run the MOC model through the entire reach. The final disadvantage of the MOC model is that the version used has no method of transferring control of propagating the leading edge of the flood wave from the shock wave equations to the gradually varied flow equations. The result of this would be loss of mass as the solution progressed because the wave continues to propagate based on an extremely small shock velocity.

Because of these problems, the IFD model was used after the shock wave had dissipated to route the flood wave through the end of the study reach and to the completion of the simulation period. The IFD model has the advantage of not being restricted by the Courant time criteria and theoretically, is stable for any time increment. However, experience using this particular model has shown that for rapidly changing flow conditions, the most accurate solution is obtained at time steps close to the Courant condition. The IFD model is also a much simpler and shorter program than the MOC model. However, the IFD program is not as versatile in that it cannot compute shock waves or supercritical flow.

To demonstrate the equivalence of the MOC and IFD models, a hypothetical 9.14-meter-high surge was propagated in a prismatic channel. The 9.14-meter surge was selected because the IFD model was stable for this height. Figure 4 shows the water-surface profiles at different times. The propagation speed cannot be expected to be exactly the same because the MOC model uses the shock wave equation to advance the surge. However, the two models are acceptably close and can be used interchangeably as long as the IFD model is stable.

Data Requirements

Both models require the same types of input data. The cross-sectional geometry must be described at each section in the reach that the geometry changes significantly. The Manning roughness coefficient is required for each cross section. The size and shape of the breach must be selected and used as input for the dam cross section. The water-surface elevation in the reservoir prior to failure must be determined. The initial conditions in the reach must be selected. Upstream boundary conditions, which is the reservoir inflow, must be determined. The downstream boundary conditions at the end of the study reach must also be selected. How these data were selected for this study will be detailed in the procedure section.

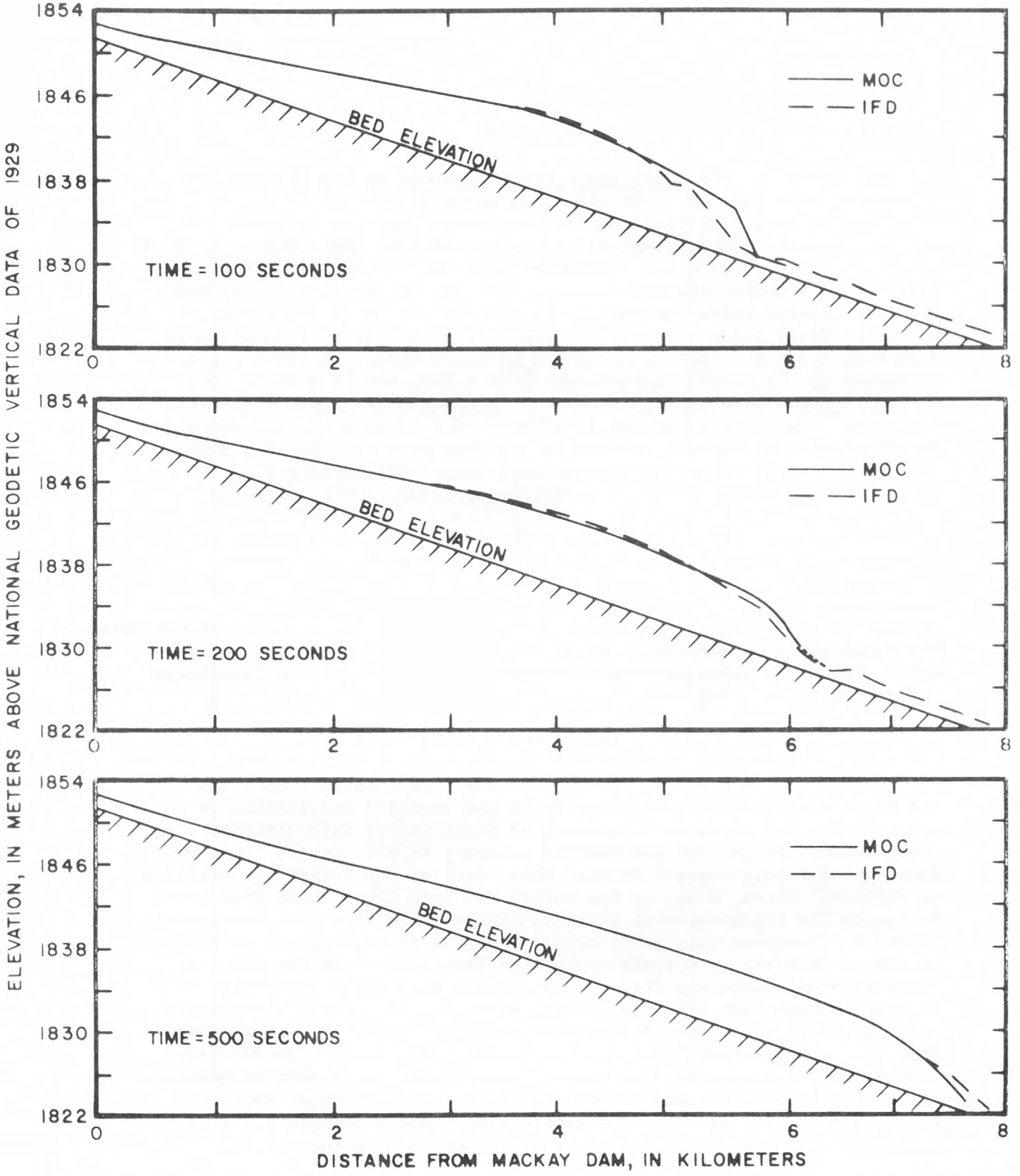

Figure 4.--Comparison of IFD (implicit finite-difference) model and MOC (method of characteristics) model for a 9.14 m hypothetical dam-break flash wave in a prismatic channel.

PROCEDURE

Site Description

All points in the study reach are referenced to the distance in kilometers from the dam. The reference point of the dam is 0.0 km. The entire reach is 114 km long. Mackay Reservoir (fig. 1) is located on the Big Lost River and is approximately 5.6 km long and averages 1,036 m wide. At full capacity the reservoir contains 54.7 hm^3 of water. Several small towns, including Mackay, Leslie, Darlington, Moore, and Arco are located below the dam. From the dam to 7.2 km downstream of Arco, the flood-plain width of the Big Lost River varies from 609 m to more than 4,572 m. Approximately 7.2 km below Arco, the flood plain converges to Box Canyon, approximately 40 m wide and 21 m deep. Box Canyon is approximately 11 km long and terminates 24 km above the INEL diversion. The INEL diversion is located 78.2 km from the dam and was constructed to alleviate flooding on the INEL site by diverting flood waters into a highly permeable spreading area. The maximum flow the diversion will convey is 62 m^3/s (Carrigan, 1972).

The places of interest on the INEL site are the Radioactive Waste Management Complex (79.7 km), State Highway 20 (86.1 km), Central Facilities Area (88.5 km), Test Reactor Area (91.7 km), Idaho Chemical Processing Plant (91.7 km), and the Naval Reactor Facility (100.6 km). Effects of the flood on the test area north of the INEL were not investigated. The flood plain on the INEL site is very flat and as much as 7,925 m wide. The study reach ends approximately 8 km above the Big Lost River playas or "sinks" (108 km).

Basic Data

Cross-section geometry information was interpolated from a small amount of field data. The objective of the geometry information is to describe how top width as a function of depth varies with distance along the channel. To provide the desired accuracy in the results, this was done approximately every 0.40 km. This level of resolution was obtained as follows. First, a map of the entire Big Lost River Basin from above Mackay to the Big Lost River Sinks was constructed from U.S. Geological Survey 7 1/2-minute quadrangle maps. Areas which appeared to be typical of the various valley terrain types were then located on the map. A field reconnaissance was then conducted, and four sites for cross-section surveys were selected. These sections are indicated in figure 1. Individual cross sections are illustrated in figures 5 to 8. Note that the cross sections are graphed on different scales. Manual and computer procedures were developed to interpolate cross section geometry at desired intervals along the channel from the four actual sections. First, a composite main channel was developed for the first 1.2 m of depth in cross-sections 1 and 2. This composite main channel was

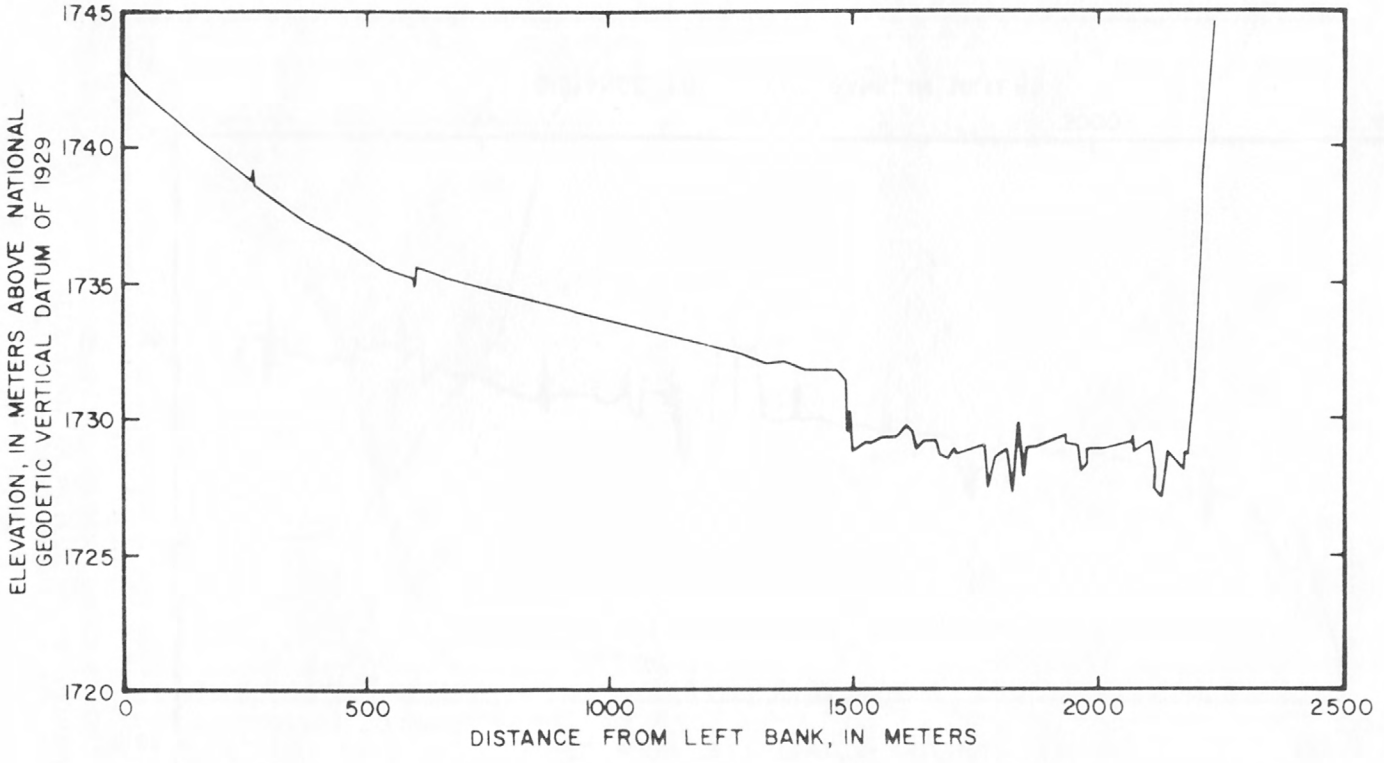

Figure 5.--Cross-section 1 surveyed near Leslie, 20.5 km from Mackay Dam.

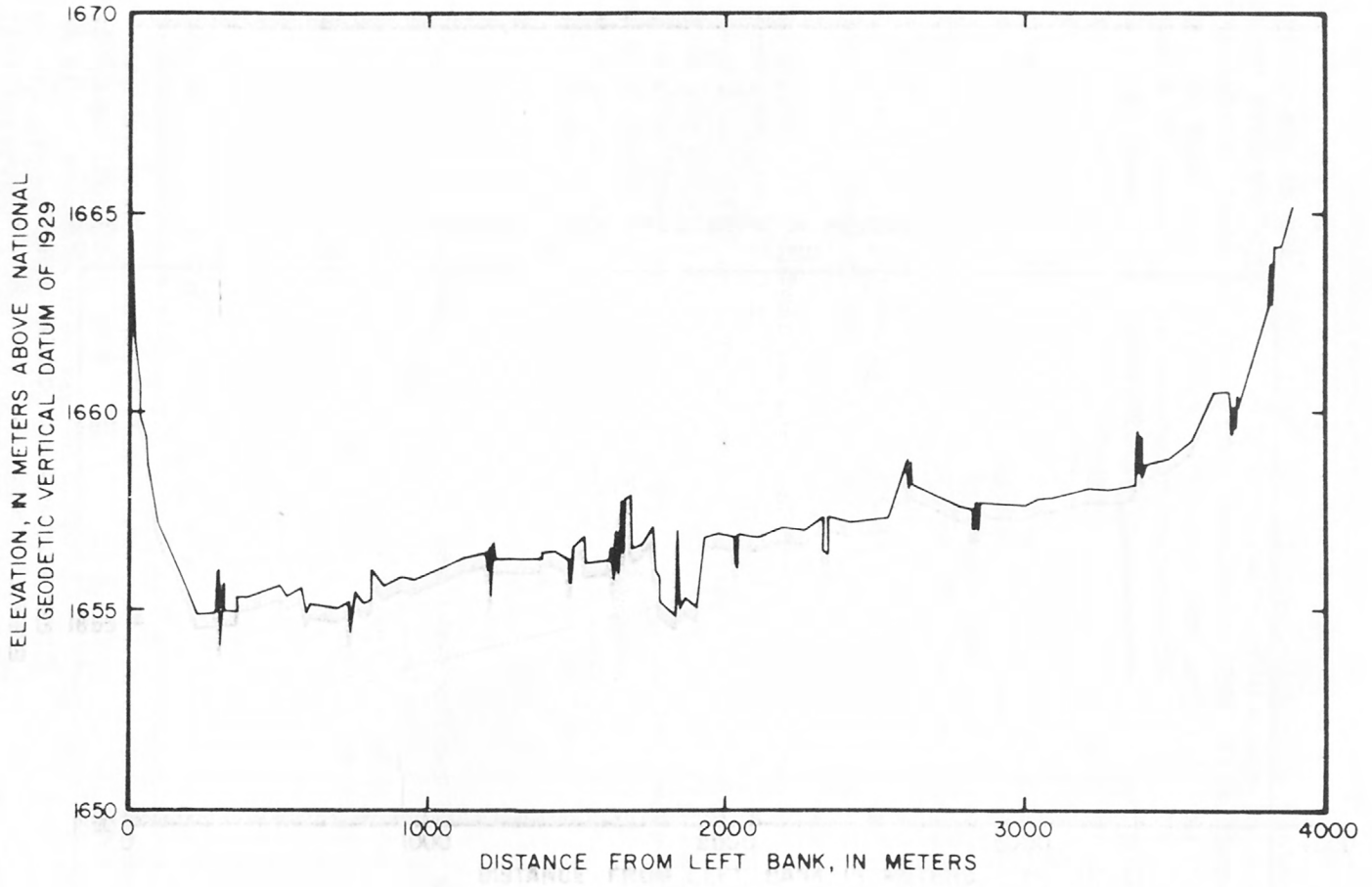

Figure 6.--Cross-section 2 surveyed near Moore, 38.6 km from Mackay Dam.

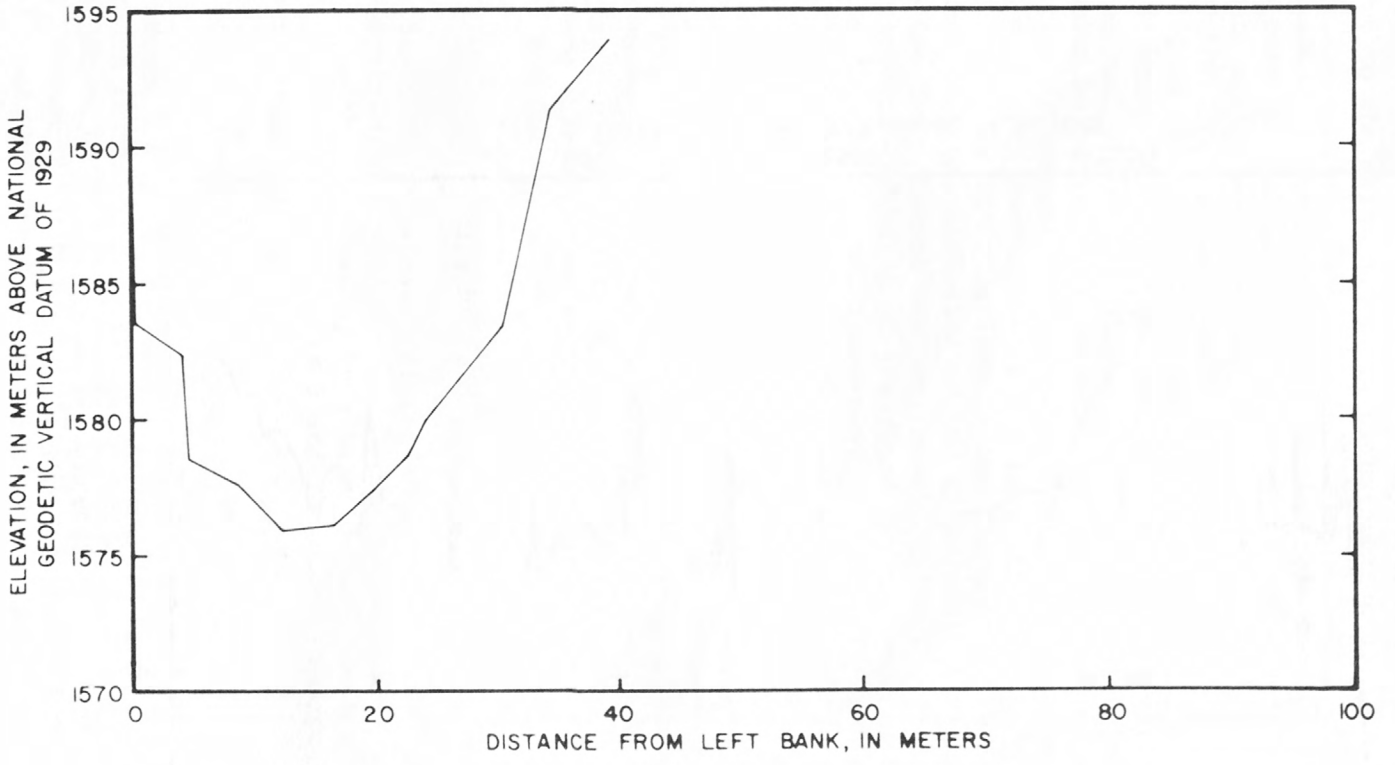

Figure 7.--Cross-section 3 surveyed in Box Canyon, 59.1 km from Mackay Dam.

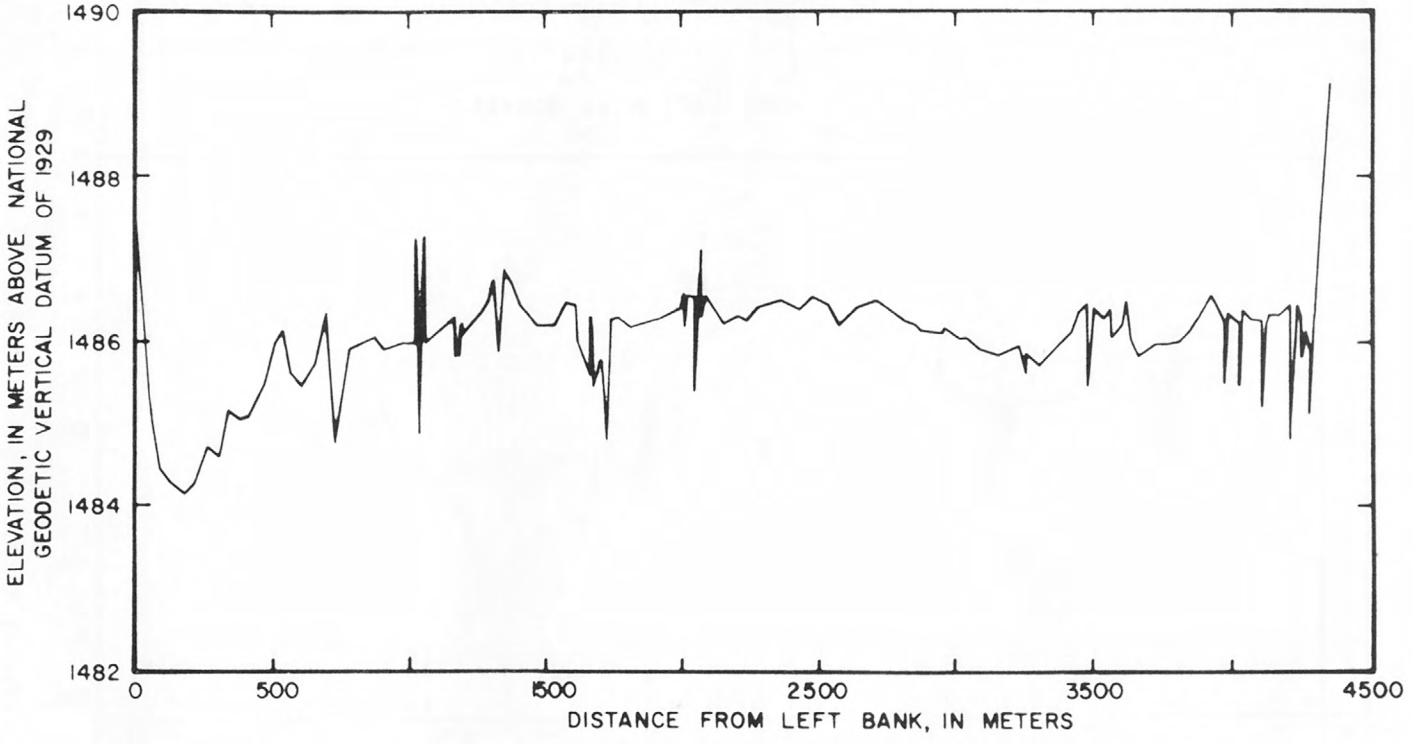

Figure 8.--Cross-section 4 surveyed near experimental dairy farm, 96.9 km from Mackay Dam.

used for all cross sections, except for Box Canyon, from the upstream boundary to the diversion. Cross-section 3 was used to describe the geometry through Box Canyon. Below the diversion, the main channel was uniformly decreased in size from the composite channel of cross-sections one and two to the main channel in cross-section 4.

Additional information to extend the cross sections from the composite main channel to the flood plain was obtained from the topographic map. First, a line was drawn down both sides of the valley at an elevation 12 m above the flood-plain elevation at the main channel. This elevation was selected as one which flood depths were not likely to exceed. Next, sections at which the valley geometry varied rapidly were identified. Examples of such places are the narrowing of the valley near Leslie, and the narrowing below Arco into Box Canyon. At each of these locations, the elevation of the channel bottom was determined. Then the slope of the flood plain was computed as being equal to the change in elevation between two contour lines divided by the distance between the two lines. The distance from the left side of the flood plain (12 m above the flood plain) to the main channel was determined, as well as the total width from the right to left side of the flood plain. These five variables (river mile, bed elevation, flood-plain slope, left-bank distance, and top width) were tabulated for each cross section. The information was used as input to an interpolation program which produced cross-section properties cards for the flow model at any interval desired. Three-dimensional plots were made of the resulting cross sections to insure that the overall shape of the river valley was preserved in the model. Cross sections representing Mackay Reservoir were obtained in the same manner; however, the mathematics were performed manually rather than by computer program for 0.40 km on either side of the dam. These cross sections were changed as necessary to simulate a complete or partial removal of the dam.

Roughness Coefficients

A detailed reconnaissance of the entire reach was made to select the Manning *n* coefficient. The *n* values varied from a low of 0.032 in the relatively smooth upper valley to a high of 0.06 for the dense sage brush on the INEL site. Figures 9 and 10 depict representative photos of the corresponding roughness elements.

Actual Size and Shape of Breach

Two breach sizes and shapes were tested for this investigation. The first one is the full breach assumed to be the removal of the entire dam. The second one is the partial breach assumed to have an arbitrary 50 percent reduction of the cross-sectional area of the full breach. The geometry of the breach can further be assumed to be an asymmetric trapezoid, as shown in figure 11, where for the partial breach the trapezoid has half of the bed width and side slopes used in describing

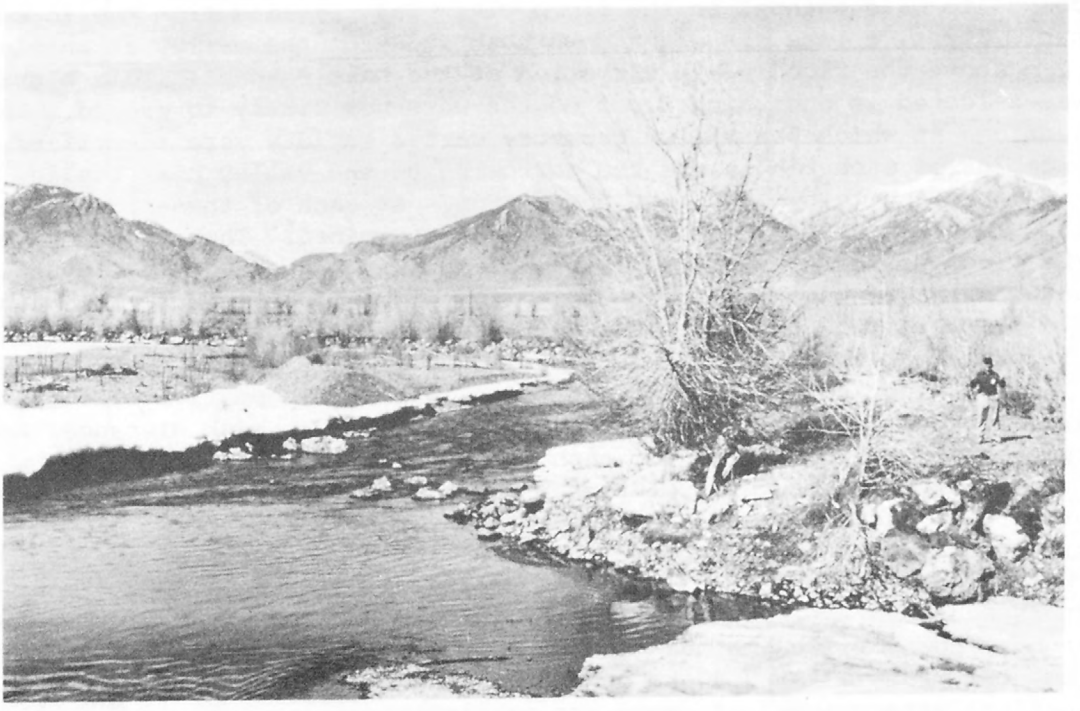

Figure 9.--Relatively smooth upper valley representing Manning's roughness coefficient of 0.032.

Figure 10.--Dense sage brush area representing Manning's roughness coefficient of 0.06.

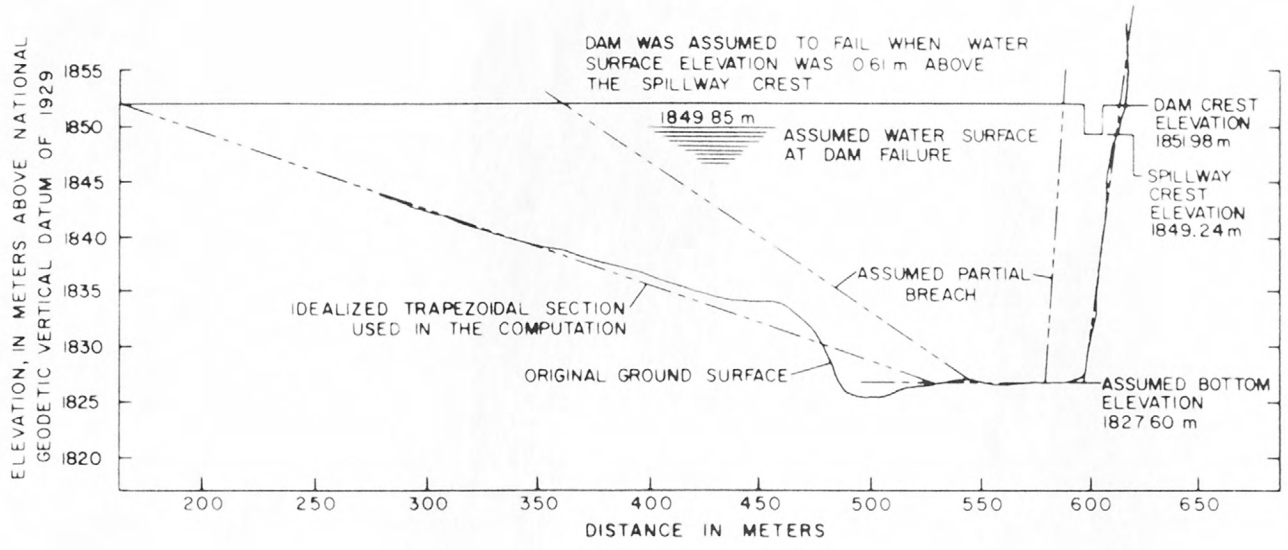

Figure 11.--The original ground-surface profile and the idealized trapezoidal cross sections used in the computations for the full breach and partial breach.

the trapezoid of the full breach. The cross-sectional area of the partial breach with this geometry will thus always possess a half of that of the full breach after the dam break.

Actual Reservoir Level

The maximum capacity of the reservoir is 54.7 hm^3. Because reservoir geometry was idealized to alleviate the computational difficulty, it was essential that the water-surface elevation at the dam at the time of the dam break be determined on the basis of this maximum capacity. The water-surface elevation so determined is 1,849.85 m which results in 22.25 m of water depth above the assumed bed elevation 1,827.60 m at the dam. This depth gives about 0.61 m above the existing spillway crest at 1,849.24 m, as shown in figure 11.

Idealized Breach and Reservoir Levels

In order for the IFD model to compute stable results, the asymmetric trapezoidal shaped breaches were replaced with symmetric trapezoids of approximately the same area. The height of the breach was set so that the reservoir capacity was 54.7 hm^3. In addition, it was necessary to smooth the actual bed surface elevations in the vicinity of the dam. These adjustments resulted in a bottom elevation of 1,824.34 m and a water-surface elevation at full reservoir capacity of 1,848.32 m. The effects of the smoothing and the symmetric trapezoid idealization were investigated with the MOC model. The results show that the discharge distribution at the time of linkage of the MOC and IFD models to be substantially the same. Therefore the idealized shapes and smoothed elevations were used in this study.

Initial and Boundary Conditions

The initial condition selected was a steady flow throughout the entire reach equal to the flood of record (85 m^3/s). The upstream boundary remained equal to the initial condition steady flow. The downstream boundary condition was a rating curve based on the steady flow equation.

Model Assumptions for this Study

Crosthwaite and others (1970) estimated the average tributary inflow to be 5.7 m^3/s. The seepage from the basin between Mackay and Arco (fig. 1) has been as great as 8.5 m^3/s and for 1959 averaged 4.3 m^3/s. Thus, the tributary inflow and seepage outflow were initially neglected since they were approximately equal. Flood-plain storage which retains water in natural or manmade depressions has the potential to intercept a large volume of flow. Removal of this water from the flood wave could greatly reduce the peak elevations and discharges in

the river. Without detailed surveys, it is impossible to account for this storage, and in this study, it initially was assumed to be zero. Any structures, such as the INEL diversion, were assumed to fail when the flood wave arrived; therefore, the resulting head losses were assumed negligible. The outflow discharge at the diversion channel was based on its maximum capacity of 62 m^3/s. The channel boundaries were assumed rigid, and no attempt was made to account for channel degradation caused by the extreme flood event.

Calculating the Dam-Break Flood

The following steps were used to calculate the dam-break flood for Mackay Dam.

Step 1. Select the steady flow and breach geometry.

Step 2. Determine the initial depths and velocities in the reservoir and river channel for use in the MOC model. The initial reservoir conditions are determined by specifying the crest elevation and using the steady, gradually varied flow equations. In the river reach, the initial conditions are determined by the uniform flow equation.

Step 3. Run the MOC model until the shock wave resulting from the dam break has dissipated, and the flow in the reach is subcritical.

Step 4. Use the velocities and depths resulting from step 3 as initial conditions in the IFD model and route the flood wave through the end of the study reach.

Step 5. For the selected sites of interest, compute the elevation and discharge hydrograph and arrival time of the leading edge of the flood wave.

These steps were completed for a steady flow of 85 m^3/s and for both a complete and a 50 percent partial failure of the dam.

Calculating the Dam-Break Flood with Infiltration

An attempt was made to represent a less severe case by calculating the full breach flood with infiltration.

Infiltration rate varies with the hydraulic head, temperature, viscosity, turbidity, duration of period of channel wetting, soil moisture content, and other factors. Based on a study of all the data available, infiltration rates were estimated (J. T. Barraclough, written commun., 1978) for use in the model to help simulate the approximate infiltration losses that might be expected if Mackay Dam fails.

Sensitivity Analysis

Because of the complexity of the controlling equations, the numerical technique and physical conditions, it is almost impossible to calculate how a mathematical model of a specific situation will respond to a change in input data. This necessitates an analysis which varies the input data and notes how the model responds. If the physical input data is varied over the range of assumed collection error, the analysis will provide an indication of the accuracy bounds for the model output. The analysis will also show the stability of the model and whether or not the model is excessively sensitive to a particular input parameter. This type of analysis is particularly important in a dam-break simulation where it is not possible to calibrate or verify the model.

The analysis is accomplished by varying the physical and numerical parameters individually and noting the change in model output. In this particular analysis the physical parameters varied will be the cross-sectional property and the roughness coefficients. The numerical parameter to be varied is the diffusive weighting factor.

The sensitivity analysis was conducted for an increase and a decrease in each parameter for a full breach. These individual variations were made on the model from above the reservoir to below the town of Moore (38.6 km). The cross sections at the towns of Mackay (7.2 km), Leslie (20.5 km), Darlington (27.4 km), and Moore (38.6 km) were selected to study the resulting output of the analysis. A composite variation of the most sensitive parameters that would provide the largest change in conditions at the INEL diversion (78.2 km) were selected and the dam breach routed through the diversion.

The variation of the physical parameters was based on the authors' estimate of the probable error in the data. The cross-sectional properties are derived from a depth versus top width relation for each section in the study reach. All top widths in the study reach were increased and decreased by 15 percent, which in turn caused the cross-sectional properties to change proportionally. The roughness coefficient was increased by 25 percent and decreased by 10 percent for all sections in the reach. The decrease was not equal to 25 percent because the model was not stable when the roughness value was decreased beyond 10 percent. This instability which was caused by decreasing the roughness coefficient was mathematically similar to the instability from the rapidly varied flow that occurred without the use of the weighting factor. The numerical parameter of α (weighting factor = 0.5) was increased and decreased by 50 percent.

The output variables to be studied were the arrival time of the leading edge and the peak depths. Peak depth was used because the relative variation for depth is more sensitive than relative variation of absolute elevation. Table 1 presents the output variables as calculated in the model for the flood of record (85 m^3/s base condition)

Table 1.--Arrival time of the leading edge, peak water-surface elevation and peak depth for full breach dam failure as calculated (A) in the model base conditions and (B) in the sensitivity analysis

A. Model base condition

Location	Distance from dam, in kilometers	Cross-section width, in meters at a depth of 6.1 m	Bed elevation, in meters	Arrival time, in hours	Peak elevation, in meters	Peak depth[1], in meters
Mackay	7.2	2,100	1,795.0	0.10	1,799.8	4.8
Leslie	20.5	2,000	1,731.3	.83	1,735.5	4.2
Darlington	27.4	3,900	1,705.7	1.4	1,709.0	3.3
Moore	38.6	4,300	1,665.7	2.4	1,668.7	3.0

B. Sensitivity analysis

Location	Arrival time, in hours	Peak elevation, in meters	Peak depth, in meters	Arrival time, in hours	Peak elevation, in meters	Peak depth, in meters
	Increasing Manning *n* 25 percent			Decreasing Manning *n* 10 percent		
Mackay	0.10	1,799.8	4.8	0.10	1,799.6	4.6
Leslie	.92	1,735.5	4.2	.83	1,735.5	4.2
Darlington	1.5	1,708.9	3.2	1.33	1,709.1	3.4
Moore	2.6	1,668.6	2.9	2.2	1,668.7	3.0
	Increasing cross-section top width 15 percent			Decreasing cross-section top width 15 percent		
Mackay	0.10	1,799.8	4.8	0.10	1,799.7	4.7
Leslie	.86	1,735.4	4.1	.83	1,735.5	4.2
Darlington	1.5	1,708.9	3.2	1.4	1,709.0	3.3
Moore	2.6	1,668.6	2.9	2.4	1,668.7	3.0
	Increasing weighting factor α to 0.75			Decreasing weighting factor α to 0.25		
Mackay	0.10	1,799.6	4.6	0.10	1,799.3	4.8
Leslie	.8	1,735.3	4.0	1.0	1,735.7	4.4
Darlington	1.2	1,708.9	3.2	1.6	1.709.3	3.6
Moore	2.1	1,668.6	2.9	2.5	1,668.9	3.2

[1]Peak depth = peak elevation - bed elevation.

and for the individual variation of the parameters in the sensitivity analysis. For each variation, the relative change from the base condition is given as a percentage. These are shown in table 2. Neither of the output variables are overly sensitive to the individual variation of the three input parameters. The change in peak depth was the least sensitive with a maximum variation of 9 percent. Arrival time was slightly more sensitive, with a maximum variation of 20 percent. The 20-percent variation was in decreasing α to 0.25 and the trend was for less sensitivity as the wave moved downstream. In general, the output variables decreased as the wave traveled downstream. The exception was when top width was increased 15 percent, the arrival time of the leading edge occurred later. After 38 km the arrival time with increased top width had changed by 8 percent. It is reasonable to assume that the change would continue uniformly and possibly be as high as 16 percent at the diversion. However, even this amount would not be considered excessive considering that it is close to the 15 percent variation in the input parameter.

Since the arrival time was the most sensitive variable, the input parameters tested were selected for the composite analysis to result in the maximum increase and decrease in arrival time. For the maximum increase in arrival time, the roughness coefficient was increased by 25 percent, the top width was increased by 15 percent, and the weighting factor (α) was decreased to 0.25. For the maximum decrease in arrival time, the roughness coefficient was decreased by 10 percent, the top width was decreased by 15 percent, and the weighting factor (α) was increased to 0.75. It should be noted that for the first conditions, the change in peak depth will be compensating. With these changes, new initial conditions were generated for the model, and the full breach dam failure was routed to 4.2 km above the diversion and compared to the base conditions. Table 3 presents the results of this composite variation for the four cross sections used in the individual parameter sensitivity analysis and the cross section 4.2 km above the diversion. This cross section was used because it is far enough upstream from the diversion to be unaffected by the radical geometry variations that caused the data below the diversion to be of poor quality. More discussion on the data below the diversion will follow in the results section. Table 4 shows the relative change in arrival time and peak depth from model results and the composite sensitivity analysis.

The composite variation runs did not produce any relative differences on peak depth greater than 10 percent. This value will be used as a guide to the accuracy of the peak depth data above the diversion. The arrival time is sensitive to the composite variations with a relative variation of over 100 percent, 7.2 km below the dam. However, as the wave progresses downstream, the relative variation decreases, and by the time it reaches the point 4.2 km above the diversion, the error is -15 to +33 percent. These values will be used as a guide to the accuracy of the arrival time above the diversion.

Table 2.--Relative change in arrival time of leading edge and peak depth for full breach dam failure from sensitivity analysis

Location	Change in arrival time of leading edge, in percent	Change in peak depth, in percent	Change in arrival time of leading edge, in percent	Change in peak depth in percent
	Increasing Manning *n* 25 percent		Decreasing Manning *n* 10 percent	
Mackay	0	0	0	-4
Leslie	11	0	0	0
Darlington	7	-3	-5	3
Moore	8	-3	-8	0
	Increasing cross-section top width 15 percent		Decreasing cross-section top width 15 percent	
Mackay	0	0	0	-2
Leslie	4	-2	0	0
Darlington	7	-3	0	0
Moore	8	-3	0	0
	Increasing weighting factor α to 0.75		Decreasing weighting factor α to 0.25	
Mackay	0	-4	0	0
Leslie	-4	-5	20	5
Darlington	-14	-3	14	9
Moore	-13	-3	4	7

Table 3.--Arrival time of the leading edge, peak water-surface elevation, and peak depth for full breach dam failure as calculated (A) in the model base conditions and (B) in the composite sensitivity analysis

A. Model base condition

Location	Distance from dam, in kilometers	Cross-section width, in meters at a depth of 6.1 m	Bed elevation, in meters	Arrival time, in hours	Peak elevation, in meters	Peak depth[1], in meters
Mackay	7.2	2,100	1,795.0	0.10	1,799.8	4.8
Leslie	20.5	2,000	1,731.3	.83	1,735.5	4.2
Darlington	27.4	3,900	1,705.7	1.4	1,709.0	3.3
Moore	38.6	4,300	1,665.7	2.4	1,668.7	3.0
Above diversion	74.0	1,400	1,547.5	6.1	1,550.3	2.8

B. Composite sensitivity analysis

	Run 1: Increase Manning *n* 25 percent; Increase top width 15 percent; Decrease α to 0.25			Run 2: Decrease Manning *n* 10 percent; Decrease top width 15 percent; Increase α to 0.75		
Location	Arrival time, in hours	Peak elevation, in meters	Peak depth, in meters	Arrival time, in hours	Peak elevation, in meters	Peak depth, in meters
Mackay	0.21	1,800.1	5.1	0.10	1,799.7	4.7
Leslie	1.2	1,735.7	4.5	.7	1,735.4	4.1
Darlington	2.0	1,709.2	3.6	1.1	1,708.9	3.2
Moore	3.3	1,668.8	3.2	1.9	1,668.6	2.9
Above diversion	8.1	1,550.4	2.9	5.2	1,550.2	2.7

[1]Peak depth = peak elevation - bed elevation

Table 4.--Relative change in arrival time of leading edge and peak depth for full breach dam failure from the composite sensitivity analysis

Location	Run 1: Increase Manning *n* 25 percent, Increase top width 15 percent, Decrease α to 0.25		Run 2: Decrease Manning *n* 10 percent, Decrease top width 15 percent, Increase α to 0.75	
	Change in arrival time of leading edge, in percent	Change in peak depth, in percent	Change in arrival time of leading edge, in percent	Change in peak depth, in percent
Mackay	110	6	0	-2
Leslie	45	7	-16	-2
Darlington	43	9	-21	-3
Moore	38	7	-21	-3
Above diversion	33	4	-15	-4

The results of the sensitivity analysis indicate that the dam-break model is not sensitive to individual variation of the input parameters and is not overly sensitive to the composite variation.

DISCUSSIONS OF RESULTS

The mathematical model was used to compute water-surface elevation and discharge at each cross section in the study reach for each time step. The following are of practical value in dam-break modeling. The arrival time of the leading edge of the wave, maximum water-surface elevation, and the duration of flooding as indicated by the water-surface elevation hydrograph. Eight sites of interest were selected to present these data for the fully and partially breached dam.

Figure 12 presents the arrival time of the leading edge as a function of distance through the study reach. The arrival time was determined by noting the time at which the water surface started to rise above steady flow at each of the sites of interest. Figures 13 to 20 display the water-surface elevation hydrographs for the eight selected sites. From these hydrographs the maximum water-surface elevation and the time duration of flooding can be determined. Subtracting the bed elevation from the water-surface elevation will determine the depths at the sites of interest. The bed elevation is taken to be the elevation of the lowest point on the cross section.

Table 5 presents the sites of interest, the distance of the sites in kilometers from the dam, bed elevation, maximum water-surface elevation, maximum discharge, the arrival time, and time of peak. Data for other sections in the study reach are available.

Table 6 presents a comparison of the results obtained when infiltration rates were used in the calculation of the full breach flood.

The usual procedure in mathematical modeling includes calibration of the model, verification with an independent data set, and simulation of the required event. This procedure cannot be followed in dam-break modeling because the event greatly exceeds any previous flood, and the first two steps must be deleted. In the simulation of the required event, we can test the following:

1. Does the model conserve mass?

2. Does the model dissipate energy as the wave moves downsteam, that is, for each time step does the total energy line decrease with distance downstream?

The model results presented satisfy the above criteria.

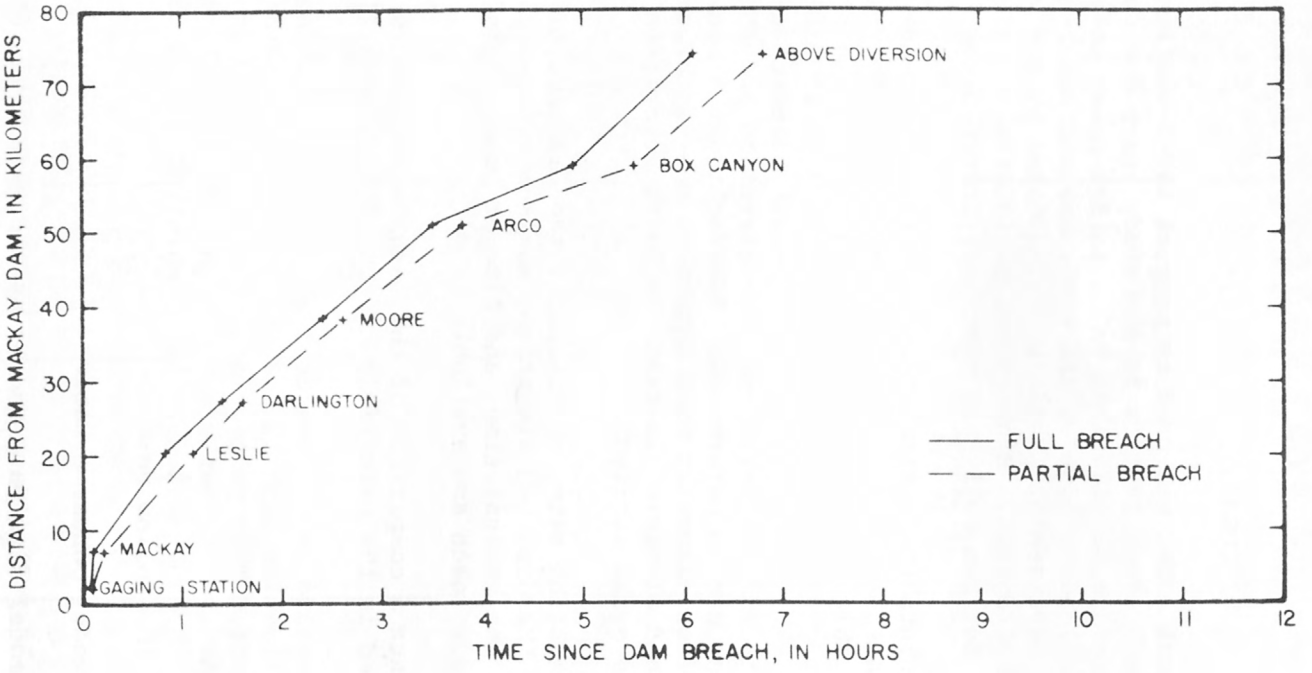

Figure 12.--Time of arrival of leading edge of the wave.

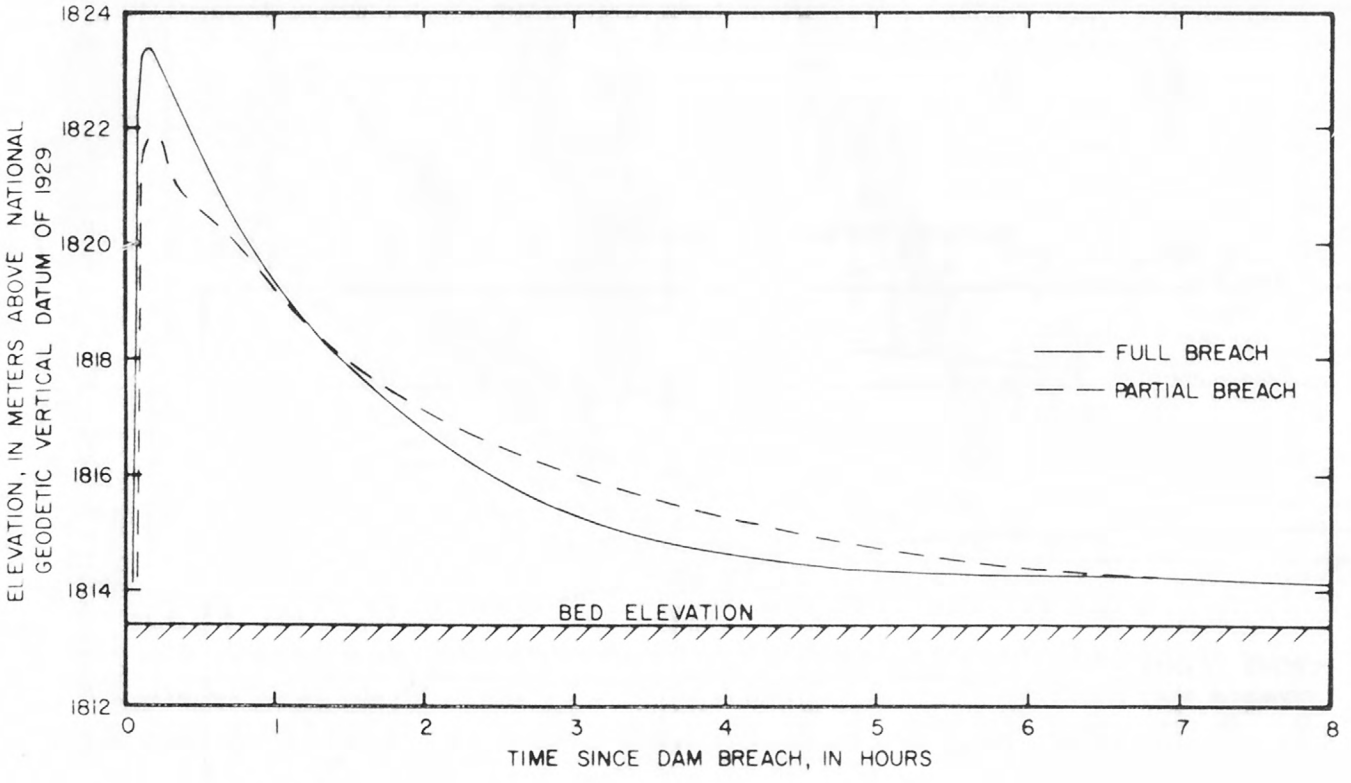

Figure 13.--Water-surface elevation hydrograph for Gaging Station, Idaho, 2.4 km from the dam.

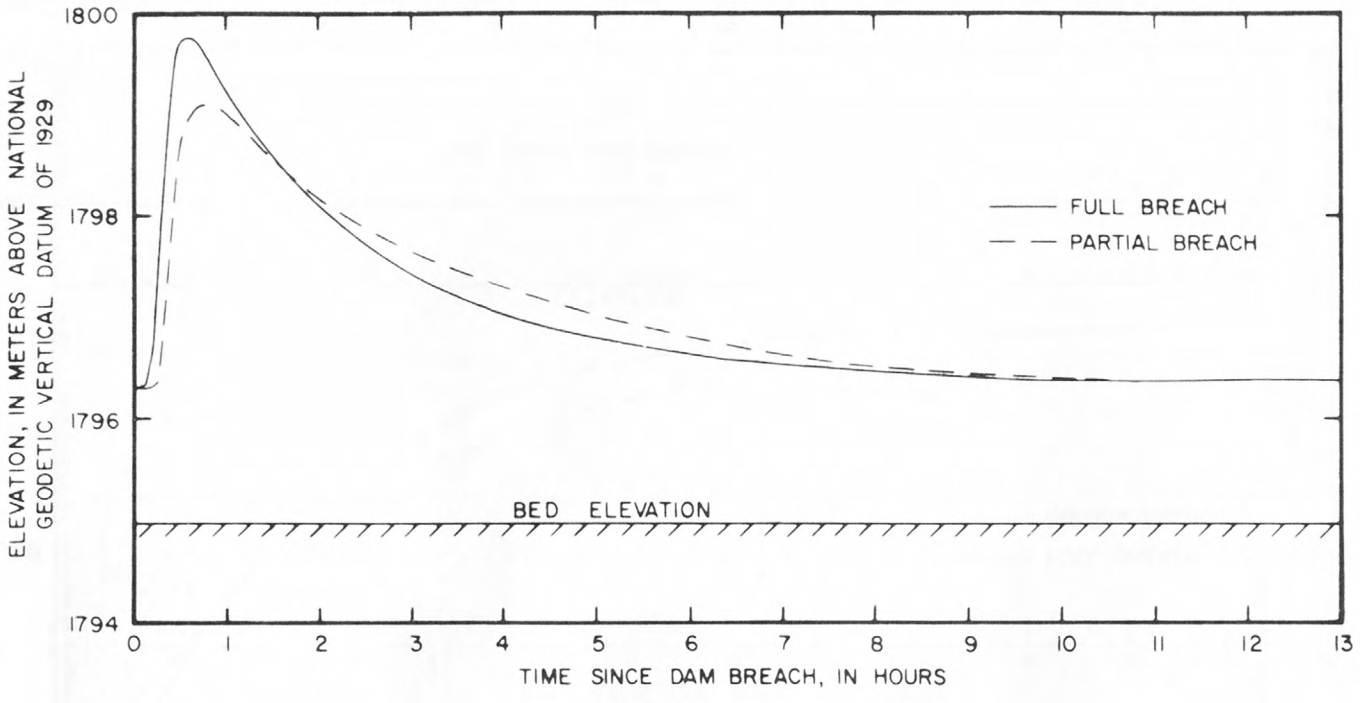

Figure 14.--Water-surface elevation hydrograph for Mackay, Idaho, 7.2 km from the dam.

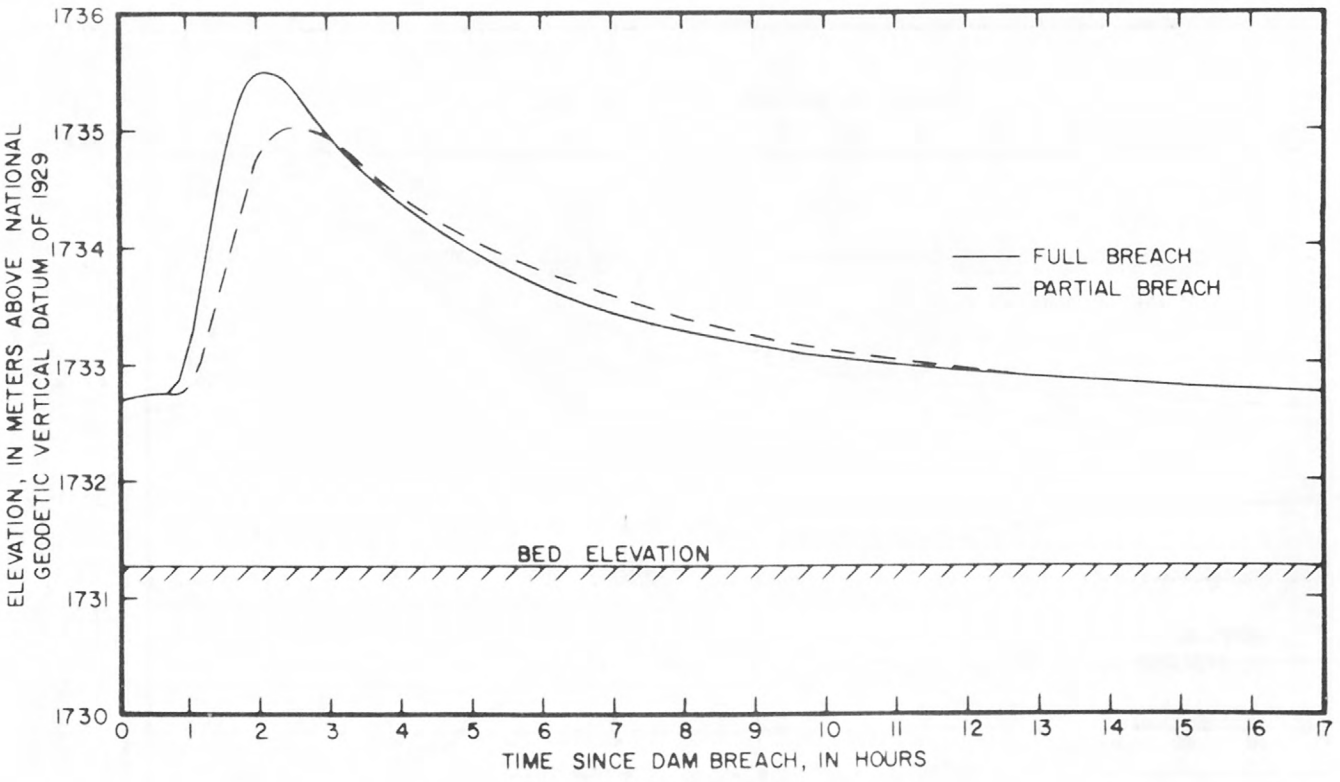

Figure 15.--Water-surface elevation hydrograph for Leslie, Idaho, 20.5 km from the dam.

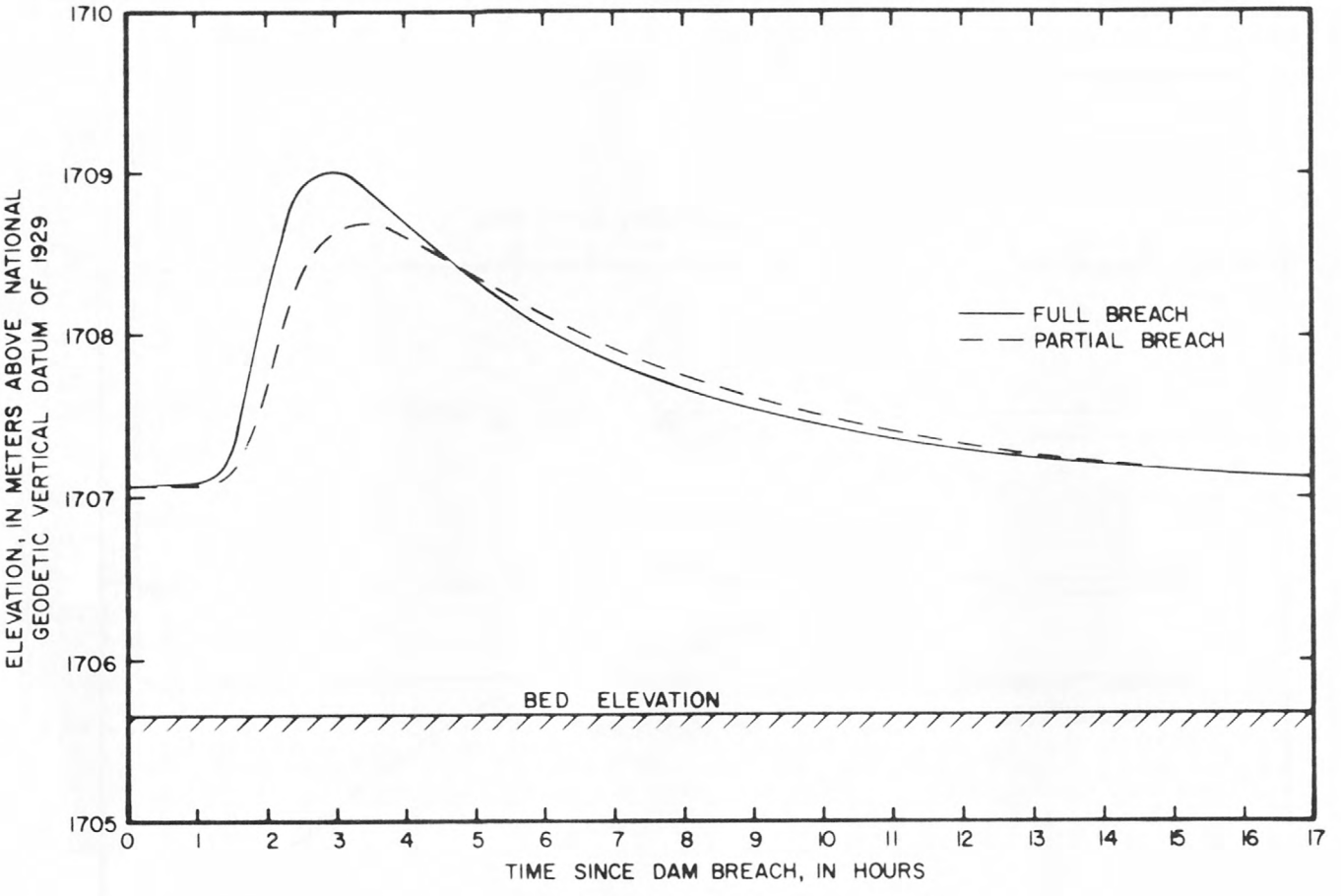

Figure 16.--Water-surface elevation hydrograph for Darlington, Idaho, 27.4 km from the dam.

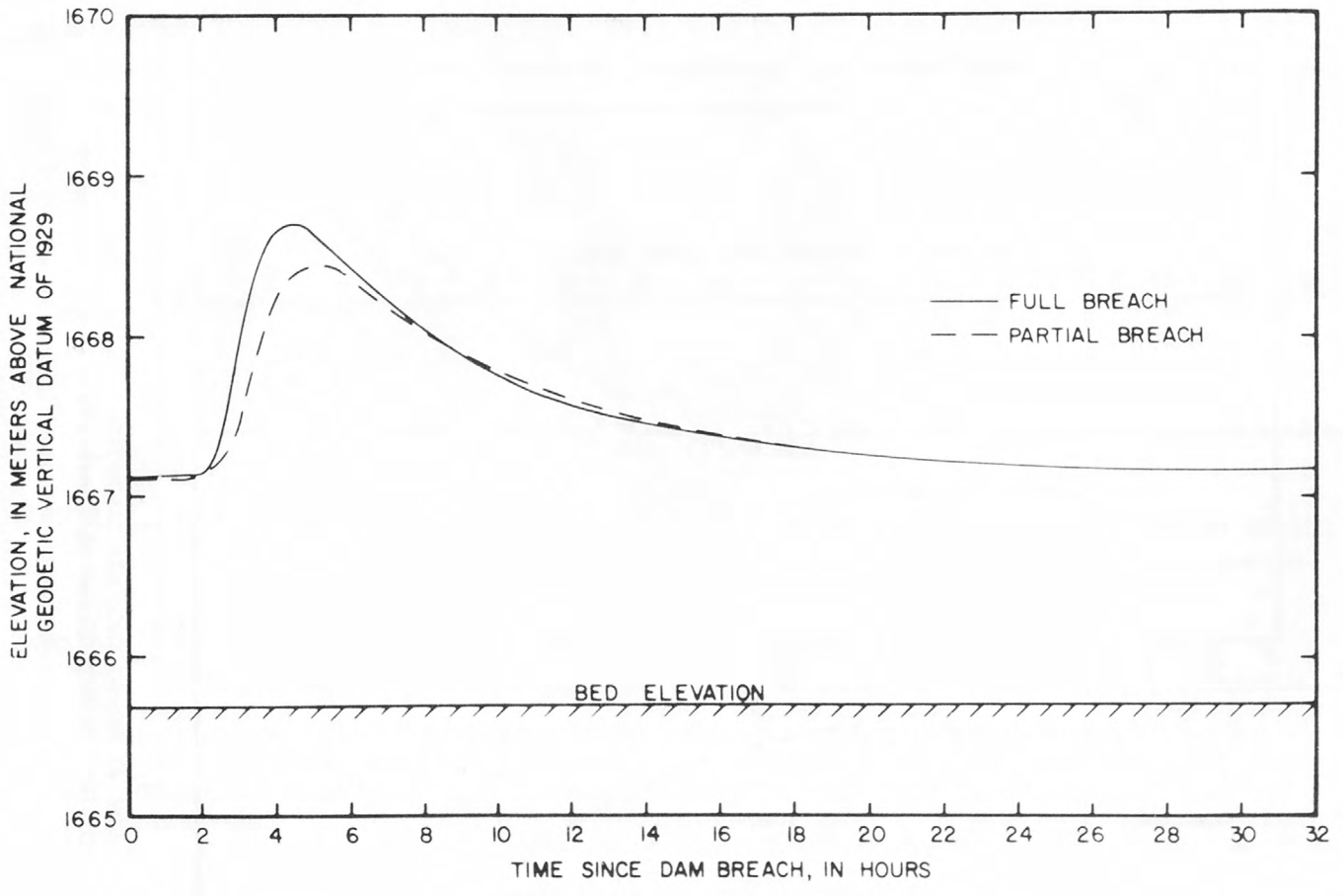

Figure 17.--Water-surface elevation hydrograph for Moore, Idaho, 38.6 km from the dam.

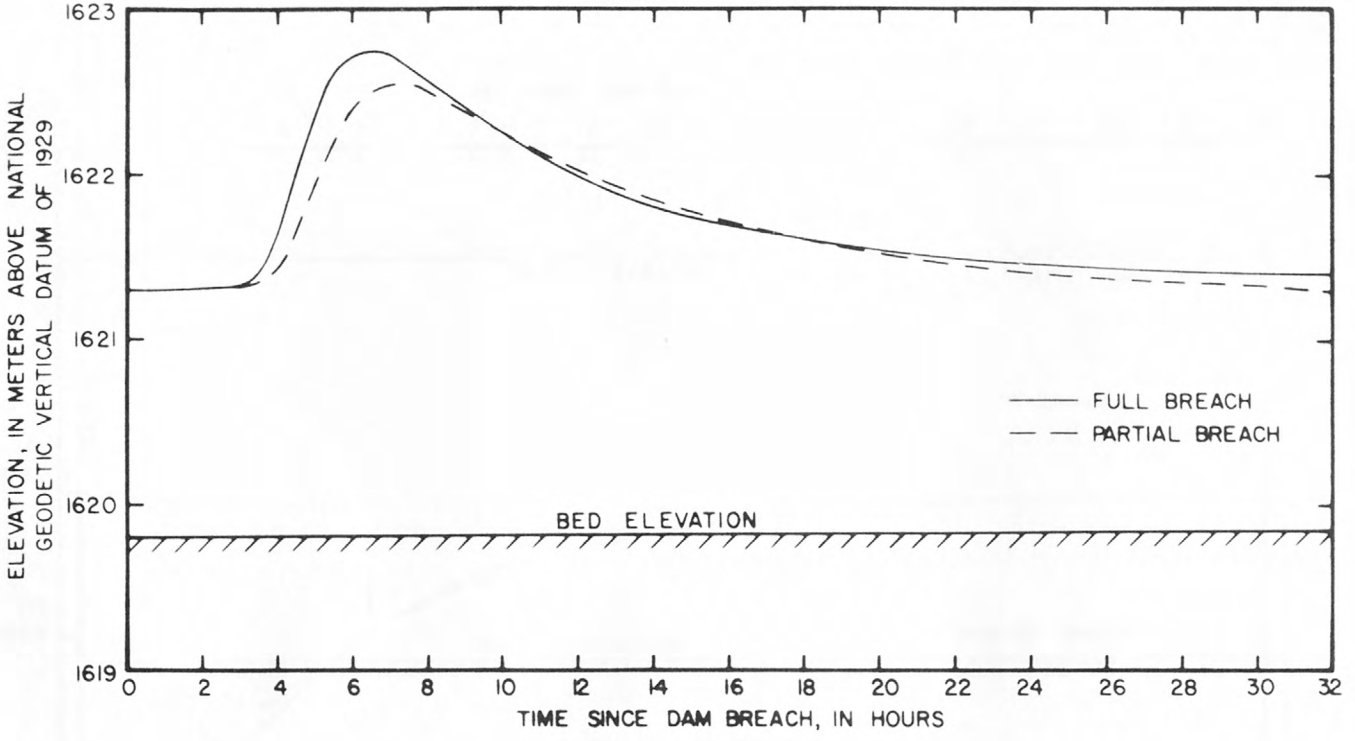

Figure 18.--Water-surface elevation hydrograph for Arco, Idaho, 51.1 km from the dam.

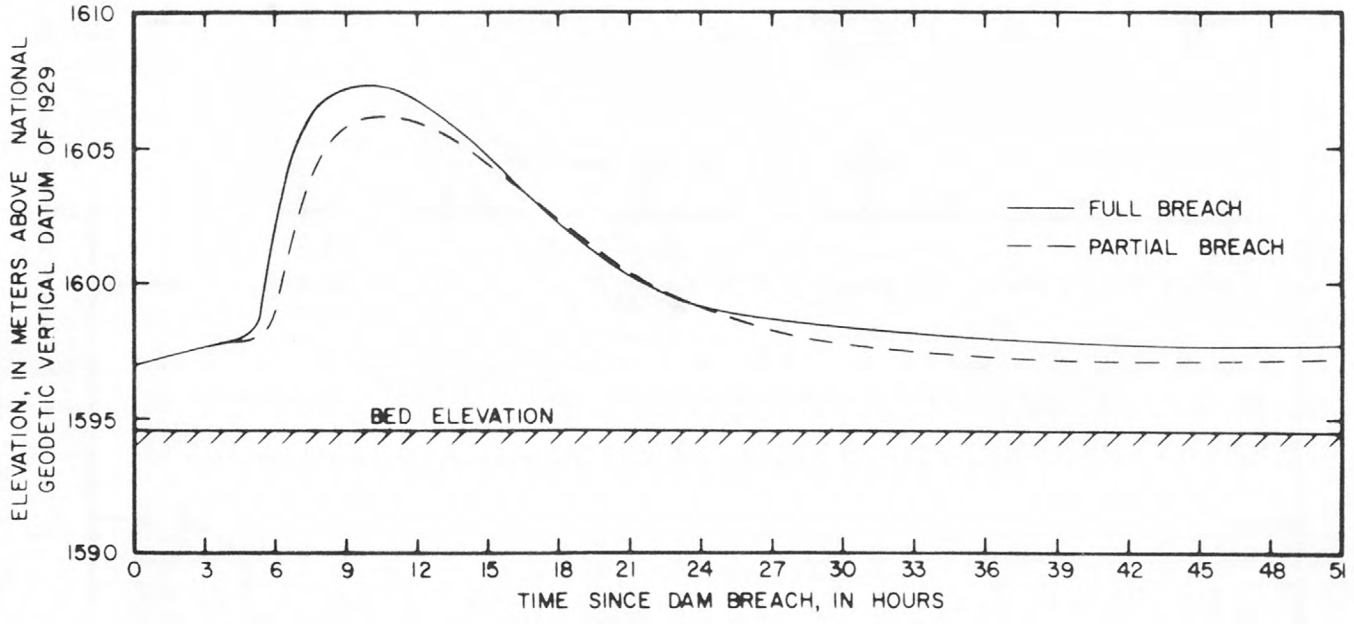

Figure 19.--Water-surface elevation hydrograph for Box Canyon, Idaho, 59.1 km from the dam.

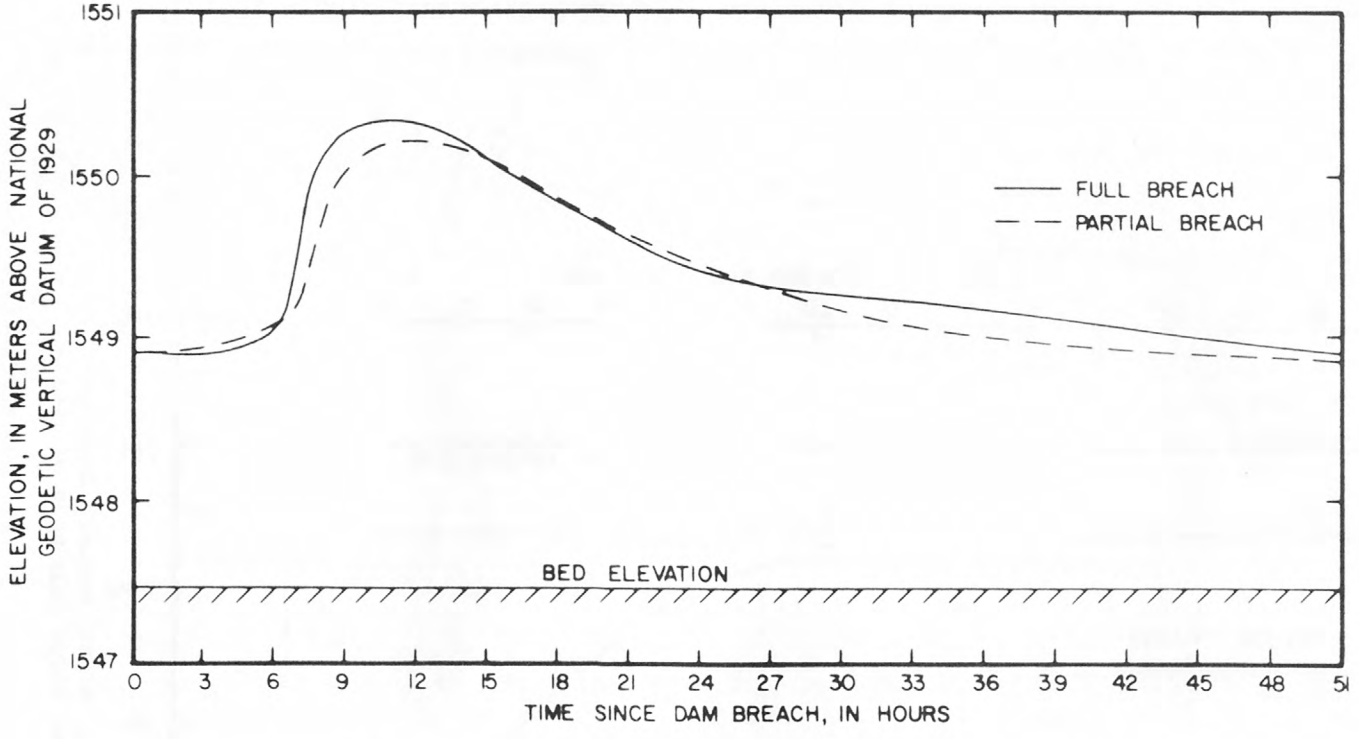

Figure 20.--Water-surface elevation hydrograph for above INEL Diversion, Idaho, 74.0 km from the dam.

Table 5.--Peak elevation, peak discharge, time of peak, and arrival time at each site for full and partial breaches

Model site	Model kilometer	Bed elevation, in meters	Peak elevation[1], in meters		Peak discharge, in cubic meters per second		Time of peak, in hours		Arrival time of leading edge, in hours	
			Full	Partial	Full	Partial	Full	Partial	Full	Partial
Gaging station	2.4	1,813.4	1,823.4	1,821.8	19,054	11,654	0.12	0.24	0.07	0.09
Mackay	7.2	1,795.0	1,799.8	1,799.1	11,427	6,771	.54	.74	.10	.20
Leslie	20.5	1,731.3	1,735.5	1,735.0	6,625	4,509	2.0	2.4	.83	1.1
Darlington	27.4	1,705.7	1,709.0	1,708.7	3,984	2,732	2.9	3.3	1.4	1.6
Moore	38.6	1,665.7	1,668.7	1,668.4	3,517	2,490	4.4	5.0	2.4	2.6
Arco	51.1	1,619.8	1,622.8	1,622.6	2,551	1,871	6.4	7.1	3.5	3.8
Box Canyon	59.1	1,594.5	1,607.3	1,606.2	1,527	1,304	8.9	9.8	4.9	5.5
Above diversion	74.0	1,547.5	1,550.3	1,550.2	1,502	1,275	10.6	11.5	6.1	6.8

[1]Peak depth = peak elevation - bed elevation.

Table 6.--Comparison of peak elevation, peak discharge, time of peak, and arrival time at each site for full breach run without infiltration and with infiltration calculated

Model site	Model kilometer	Bed elevation, in meters	Peak elevation[1], in meters		Peak discharge, in cubic meters per second		Time of peak, in hours		Arrival time of leading edge, in hours	
			Infiltration		Infiltration		Infiltration		Infiltration	
			Without	With	Without	With	Without	With	Without	With
Gaging station	2.4	1,813.4	1,823.4	1,823.4	19,054	19,041	0.12	0.12	0.07	0.07
Mackay	7.2	1,795.0	1,799.8	1,799.8	11,427	11,318	.54	.54	.10	.10
Leslie	20.5	1,731.3	1,735.5	1,735.5	6,625	6,165	2.0	2.0	.83	.83
Darlington	27.4	1,705.7	1,709.0	1,709.0	3,984	3,500	2.9	2.9	1.4	1.4
Moore	38.6	1,665.7	1,668.7	1,668.5	3,517	2,772	4.4	4.4	2.4	2.4
Arco	51.1	1,619.8	1,622.8	1,622.5	2,551	1,560	6.4	6.4	3.5	3.5
Box Canyon	59.1	1,594.5	1,607.3	1,604.5	1,527	951	8.9	8.7	4.9	5.0
Above diversion	74.0	1,547.5	1,550.3	1,550.0	1,502	833	10.6	10.1	6.1	6.8

[1]Peak depth = peak elevation - bed elevation.

In judging how reasonable the results are, the basic data and model assumptions must be considered. The basic data such as cross-section properties and roughness coefficients were assembled with care and should be satisfactory. Initially, an attempt was made to calculate the flood wave for the worst possible case. The assumptions of instantaneous dam failure, no depression storage, no head losses from structures in the flood plain, and no infiltration, all make the flood event more severe. A run was made to include infiltration rates to represent a less severe case.

It is difficult to quantify the effects of these assumptions. However, a sensitivity analysis was conducted which evaluated the effects of changing valley geometry, roughness coefficients, and the diffusive weighting factor. The results shown in tables 1-4 indicate that varying these factors had little effect on the answer. Therefore, the assumptions can be considered valid.

The absolute accuracy of the times and elevations presented are difficult to determine. Drawing from the results of the sensitivity analysis and a knowledge of the physical conditions, the following accuracy limits were developed. The peak depths above the diversion are within $\pm$10 percent. The variation in wave arrival time above the diversion ranges from over +100 percent close to the dam to about $\pm$30 percent at the diversion. The accuracy of the arrival times between these points varies proportionally to the distance downstream. The accuracy of the peak water-surface elevations, arrival times, and peak discharges below the diversion was very poor. As a result these numbers have not been included in this report. The reach below the diversion is characterized by shallow depths with several extreme expansions and contractions and several reaches with widths in excess of 7,315 m. These conditions are poorly simulated by a one-dimensional model such as the one used. In addition, because of the apparently complex flood-plain geometry and the lack of detailed ground-surface elevations in the vicinity of the diversion, it was not possible to determine where the flood wave would go. In order to route the flood wave from the diversion to INEL, additional cross sections are needed. A flood inundation map could be drawn on a topographic map with a 0.3 m contour interval. Should a two-dimensional flow model be needed, this same topographic map could be used to establish the boundary geometry.

There will be flooding throughout the study reach and there appears to be no appreciable difference in the full and partial breach failure. In the reach from the dam to the diversion, the elevation hydrographs give a good indication of the magnitude of flooding. To determine the defenses required at any point, the elevation of that point should be compared to the maximum elevation of the hydrograph. However, care must be used in doing this because the elevations in the model were approximated from a topographic map and may not be the same as a surveyed elevation.

If this is the case, use the maximum depth as a guide to the severity of the flooding. Immediately below the diversion, part of the flow will undoubtedly leave the main channel and adjacent flood plain and progress towards the RWMC. The magnitude of the flooding at the RWMC is impossible to determine with the data available, but with the assumptions made in this study, it will almost certainly occur. A best estimate of the order of magnitude of the peak wave at RWMC could occur if the peak calculated at 4.2 km above the diversion was translated to the RWMC without further attenuation.

Table 6 shows the effect that calculating the flood wave with infiltration has on the study sites. There were no changes in the values from Gaging Station (2.4 km) to Darlington (27.4 km). From Moore (38.6 km) to the end of the study reach (100.6 km) the change in peak elevation ranged from -0.2 to -1.0 m. The peak elevation above the diversion (74.0 km) dropped 0.3 m. At this location, the peak discharge calculated with infiltration was 833 m^3/s, a decrease of 669 m^3/s.

Depression storage was not included in the mathematical model. It is difficult to measure in the field as well. For engineering purposes, the following comparisons may be useful in estimating the possible effect of depression storage. The area of the flood plain that would be wetted by the flood wave is 20,672 ha. If the initial volume of the reservoir (54.7 hm^3) would be uniformly distributed across the flood plain, the depth would be 0.26 m. After routing the flood wave with infiltration for the full breach, the volume at 4.2 km above the diversion is 17.1 hm^3. If this volume were uniformly distributed on the flood plain, the depth would be only 0.083 m. In other words, about two-thirds of the water is lost to infiltration. Of the remaining one-third, it is likely that a substantial portion of this will be lost to depression storage.

CONCLUSIONS

The hypothetical failure of Mackay Dam was simulated with a mathematical dam-break model. The results for arrival time of the flood wave, peak elevation, and duration of flooding were presented for eight sites throughout this study reach. The results above the INEL diversion are considered good and will provide a reasonable indication of the timing and severity of the flooding. Below the diversion, the physical system departs radically from the one-dimensional assumptions made in the mathematical model. This resulted in a poor simulation of the hypothetical event. Consequently, these results are not presented in this report.

When infiltration and depression storage are assumed to be zero on the flood plain, the peak discharge at the diversion is 1,550 m^3/s. Adding the effects of infiltration reduces the peak discharge to 833 m^3/s. The volume of water is reduced from 54.7 hm^3 to 17.1 hm^3 or

approximately two-thirds of the water is lost to infiltration. If the remaining water were spread uniformly across the wetted flood plain, the resulting depth would be 0.083 m. Consequently, it is likely that a significant part of the remaining one-third of the water would be lost to depression storage.

RECOMMENDATION

The conservative case has been presented and the case which considers the effects of infiltration. The following peak elevation and peak discharges above the diversion were calculated: full breach (1,550.3 m, 1,502 m^3/s), partial breach (1,550.2 m, 1,275 m^3/s), and full breach with infiltration (1,550.0 m, 833 m^3/s). Obviously, infiltration has a considerable affect on the peak discharges but much less on peak elevations.

A question remains as how to obtain good results below the diversion. The following recommendation is based on the experience gained in this study.

1. Detailed topographic data are needed especially between the diversion, RWMC, and the Central Facilities Area. Since the expected flow depths are on the order of 1 or 2 m, a topographic map with at least a 0.5-m contour interval is needed. A finer scale would further improve the estimate.

2. Using the calculated peak flow at the diversion and a detailed topographic map, a steady flow analysis could be used to draw a flood inundation map of the area between the diversion, RWMC, and the Central Facilities Area. This inundation would represent a worst case estimate and provide an estimate of the maximum water-surface elevation at RWMC.

3. The detailed topographic map could be used to vastly improve the accuracy of the one-dimensional model used in this report.

4. The detailed topographic map could be used for a two-dimensional flow model if a refined analysis is needed after a steady flow flood inundation study and an improved one-dimensional flow model are attempted.

5. After the flow is routed through INEL, stage storage relations for the playas would be needed to estimate their capacity to store the flood flow. The published capacities of the playas were determined for flow volumes much lower than those that would result from a dam break.

REFERENCES

Bennett, J. P., 1975, General model to simulate flow in branched estuaries: Symposium on Modeling Techniques, 2d Annual Symposium of the Waterways, Harbors, and Coastal Engineering Division, American Society of Civil Engineers, San Francisco, California, v. 1, p. 643-662.

Carrigan, P. H., Jr., 1972, Probability of exceeding capacity of flood-control system at the National Reactor Testing Station, Idaho: U.S. Geological Survey Open-File Report, Reston, Virginia, 102 p.

Chen, Cheng-lung, 1975, Urban storm runoff inlet hydrograph study, Computer analysis of runoff from urban highway watersheds under time- and space-varying rainstorms: Logan, Utah State University, Utah Water Research Laboratory Report PRWG106-1, v. 1, 150 p.

Courant, R., Friedrichs, K. O., and Lewy, H., 1928, Uber die partiellen differenzengleichungen der mathematischen physik: Mathematische Annalen, v. 100, p. 32-74.

Crosthwaite, E. G., Thomas, C. A., and Dyer, K. L., 1970, Water resources in the Big Lost River basin, south-central Idaho: U.S. Geological Survey Open-File Report, 109 p.

Cunge, J. A., 1975, Rapidly varying flow in power and pumping canals, in K. Mahmood and V. Yevjevich, eds., Unsteady flow in open channels: Ft. Collins, Colorado, Water Resources Publication, v. II, p. 539-586.

Gundlack, D. L., and Thomas, W. A., 1977, Guidelines for calculating and routing a dam-break flood: Davis, California, U.S. Army Corps of Engineers Hydrologic Engineering Center Research Note, no. 5, 49 p.

Levin, L., 1952, Mouvement nonpermanent sur les cours d'Eau a là suite de rupture de barrage [Unsteady flow in rivers created by dam break]: Revue Générale de l' Hydraulique, Paris, no. 72, p. 297-315.

Liggett, J. A., and Cunge, J. A., 1975, Numerical methods of solution of the unsteady flow equations, in K. Mahmood and V. Yevjevich, eds., Unsteady flow in open channels: Fort Collins, Colorado, Water Resources Publication, v. I, p. 89-182.

Martin, C. S., and DeFazio, F. G., 1969, Open channel surge simulation by digital computer: American Society of Civil Engineers Proceedings, Journal of the Hydraulics Division, v. 95, no. HY6, p. 2049-2070.

Price, J. T., Lowe, G. W., and Garrison, J. M., 1974, Hydraulic transients generated by partial and total failures of large dams: American Society of Civil Engineers Specialty Conference, Knoxville, Tennessee, 11 p.

Sakkas, J. G., 1974, Dimensionless graphs of floods from ruptured dams: U.S. Army Corps of Engineers, Hydrologic Engineering Center, Davis, California, 60 p.

Stoker, J. J., 1957, Water waves, Vol. IV, Pure and applied mathematics: New York, Interscience Publishers, 567 p.

Strelkoff, Theodore, 1969, One-dimensional equations of open-channel flow: American Society of Civil Engineers Proceedings, Journal of the Hydraulics Division, v. 95, no. HY3, p. 861-875.

_____1970, Numerical solution of Saint-Venant equations: American Society of Civil Engineers Proceedings, Journal of the Hydraulics Division, v. 96, no. HYl, p. 223-253.